DEVELOPMENT OF A WEARABLE EYE TRACKER

CHUNG YUN SHENG

UNIVERSITI TUNKU ABDUL RAHMAN

DEVELOPMENT OF A WEARABLE EYE TRACKER
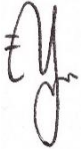
CHUNG YUN SHENG

A project report submitted in partial fulfilment of the requirements for the award of Bachelor of Biomedical Engineering with Honours

Lee Kong Chian Faculty of Engineering and Science
Universiti Tunku Abdul Rahman

September 2023

DECLARATION

I hereby declare that this project report is based on my original work except for citations and quotations which have been duly acknowledged. I also declare that it has not been previously and concurrently submitted for any other degree or award at UTAR or other institutions.

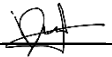|		
Signature	:	
Name	:	Chung Yun Sheng
ID No.	:	1905615
Date	:	18 September 2023

APPROVAL FOR SUBMISSION

I certify that this project report entitled **"DEVELOPMENT OF A WEARABLE EYE TRACKER"** was prepared by **CHUNG YUN SHENG** has met the required standard for submission in partial fulfilment of the requirements for the award of Bachelor of Biomedical Engineering with Honours at Universiti Tunku Abdul Rahman.

Approved by,

Signature   :

Supervisor   :   Dr Tan Lee Fan

Date   :   18 September 2023

Signature   :

Co-Supervisor :   Ir Dr Danny Ng Wee Kiat

Date   :   18 September 2023

ABSTRACT

Eye trackers provide valuable insights into visual perception and gaze behaviour. However, the high costs and restricted mobility of current devices available in the market limit broader applications. This study aimed to develop an affordable, wearable eye tracker for naturalistic settings. Low-cost hardware and 3D-printed structures were utilized in this study to ensure cost-effectiveness. Gaze detection was started from mounting headset adjustments, followed by fine-tuning in detecting pupil, calibration, data processing on recorded data, and data analysis for calibrated data. Performance evaluations demonstrated major improvements compared to a previous model, with over 50% enhancement in angular accuracy and precision and a 52% reduction in data loss. The prototype exhibited excellent angular accuracy (0.939°) and precision (0.097°) in controlled non-movement conditions. However, facial movements and expressions generated motion artefacts that increased variability in measurements. Similarly, head and eye tracker movements produced substantial deviations in accuracy, precision, and data loss due to motion artifacts and slippage effects. A colour detection plugin was also developed, demonstrating over 90% accuracy in bright and natural lighting environments. This device could assist colour-blind individuals through real-time feedback. This ongoing colour detection could possibly assist colour-blind individuals in their daily lives as well as enhance their learning process. Further advancements can be made by improving camera sensor quality, refining algorithms, adding supplemental lighting, and collecting user feedback. Detailed validation and testing on a larger participant group across real-world scenarios could enhance effectiveness across user demographics and various use cases.

TABLE OF CONTENTS

CHAPTER

LIST OF TABLES

LIST OF FIGURES

LIST OF SYMBOLS / ABBREVIATIONS

m^2	square metre
mA	milliampere
mm	millimetre
ms	millisecond
nm	nanometre
V	volt
W	Watt
Ω	ohm

2D	two-dimensional
3D	three-dimensional
ABS	acrylonitrile butadiene styrene
ACGIH	American Conference of Governmental Industrial Hygienists
API	Application Programming Interface
CT	computed tomography
ECG	electrocardiogram
EEG	electroencephalogram
FDM	fused deposition modelling
FOV	field of view
fps	frames per second
IR	infrared
I-VT	Velocity-Threshold Identification
LED	light emitting diode
PA	polyamide
PC	polycarbonate
PE	polyethylene
PLA	polylactic acid
PP	polypropylene
ROG	Republic Of Gamers
USB	Universal Serial Bus
WHO	World Health Organization

LIST OF APPENDICES

CHAPTER 1

INTRODUCTION

1.1 General Introduction

Eye tracking is the process of tracking the eye's movement to distinguish the exact location of the person looking at it and its duration (Klaib, et al., 2021). Eye trackers are devices that can measure precisely eye movements and provide valuable insights into how humans perceive, process, and respond to visual information. According to Brunye, et al. (2019), an array of infrared or near-infrared light sources and cameras are utilised to build eye tracking system. An eye tracker is able to track the gaze behaviour of one or both eyes (Holmqvist, et al., 2017). In the latest eye-tracking system, an array of non-visible light sources is directed towards the eye to produce a corneal reflection (Brunye, et al., 2019). The relationship between the reflection and pupil's centre is examined continuously by the eye tracker to work out the vector which connects eye position to locations in the observed world, as the computed point of regard in space moves when eyes move (Hansen and Ji, 2010).

With the progressive advancement in eye-tracking technology, its application is now available in almost every area of life. Most eye-tracking companies are now experts at providing an understanding of human behaviours for scientific research or business purposes. For instance, eye tracking acts as a communication pathway for disabled people who can only utilize their eyes for input. Gaze interaction requires only the eye movement of disabled individuals, and it allows them to navigate and control the computer with their eyes (Rudnicki, n.d.). Besides, eye tracking also can be implemented in improving sports performance and diagnosing and treating eye diseases in a non-invasive way. For example, Zammarchi and Conversano (2021) have concluded that eye tracking is extensively used for autism spectrum disorders, which assesses abnormalities in eye movements during face processing or viewing other social stimuli.

1.2   Importance of the Study

There are many equipment or tools available for monitoring the physiological metrics and measuring mental processing in humans, such as ECG, EEG etc. The information gathered from the tools could then provide additional understanding of emotional processing. With the technology advancements, multiple instruments can be combined and put into use with synchronized measurements across the application on subjects. As such, an eye tracker is complementary to those technologies (Biondi, 2021). A combination of eye tracker with higher or lower technologies provides both subjective and objective data which allow the user excels in the cognitive mechanisms and processes.

1.3   Problem Statement

The common eye-tracking approaches require participants to sit still in front of a computer screen and place their head on a fixed chinrest in front of a table-mounted device, which can be uncomfortable and restricts the participant's movement. The table-mounted eye tracker is troublesome when the user would like to use it at various locations, as it is not easy to transfer the device from place to place. In addition, some of the eye trackers would be bulky or heavy, resulting in unpleasant user experiences.

Besides that, the cost of a wearable eye tracker has limited its application in exploratory users. For example, low-end eye trackers are priced between RM 450 to RM 4 500, middle-end eye trackers are valued between RM 4 501 to RM 45 000, and high-end eye trackers cost more than RM 45 000 (Farnsworth, 2022a). Therefore, this situation has restricted the public from using eye trackers in their daily activities.

1.4   Aim and Objectives

To address the problems and issues faced in the previous development, this study aims to design and develop a head-mounted wearable eye tracker.

Objectives:
- To design an affordable and mobile solution that can track eye movements in naturalistic settings.
- To integrate the eye tracking algorithm as a colour detector.

- To evaluate the performance of the developed eye tracker.

1.5 Scope and Limitation of the Study

The scope of this study is to design and develop a wearable eye tracker prototype that can track eye movements in lifelike settings. Cameras will be employed together with eye tracker software for the detection of the user's pupil which is essential for gaze tracking. During the study, the cost, weight, and mechanical properties will be taken into consideration to offer an affordable alternative for individuals who are looking for a reliable eye tracker at a fair price. Besides that, the performance of the device will be evaluated based on the accuracy of the eye-tracking system.

In the development of an affordable and wearable prototype, the number of cameras is limited to a maximum of two units. More specifically, one for the eye view, and one for the front world view, where it may partially reduce the weight of the prototype can lead to better comfortability for the users. Yet, it would be better if there was one camera to capture each eye as it can provide greater accuracy and reliability of pupil detection. In addition, most of the hardware and materials selection are limited in this study as the prototype is intended to be an affordable product to the users. Moreover, the designs of the mounting platform only focus on the structural support of the frame on the nose and the ears, without concerning much about the commercial appearance of the frame as a functioning eye tracker is the main priority. Furthermore, there will be a potential for data loss due to blinking or head movement, which affects the performance of the eye tracker.

1.6 Contribution of the Study

The development of an affordable wearable eye tracker has several positive aspects across an array of fields and industries. Firstly, it improves accessibility by making eye-tracking technology broadly available. Given that eye-tracking technology is more accessible, it may be employed by researchers, teachers, and anyone with limited funds. These affordable eye-trackers have the potential to improving teaching and learning in educational settings. They support creative teaching strategies and enhance learning results, especially for children with various kinds of needs.

Low-cost eye trackers will also have a big impact on the healthcare industry. These tools can assist patients with disorders including ALS, strokes, and motor neuron diseases in recovery. Patients' overall quality of life improves significantly when they acquire control and communication skills. Additionally, affordable eye trackers are used in the field of assistive technology, enabling people with impairments to operate computers, communicate, and live more independently. Besides, the development of affordable eye-trackers fosters creativity and creates new opportunities. Such devices can encourage the development of creative software and apps, extending their usage in fresh ways and opening up new industries.

Eye trackers encourage advancement in human-computer interaction since they are affordable. They make it feasible to develop more user-friendly and engaging interfaces for devices and systems that are more natural and intuitive. Last but not least, the reduced price of eye-tracking technology stimulates market growth, competition, and innovation. This results in more people having access to more advanced and functional eye-tracking technologies, which ultimately changes how individuals utilise and benefit from this technology.

1.7   Outline of the Report

First of all, Chapter 1 will provide a general introduction to the wearable eye tracker, the importance of the study, and the problem statement. Additionally, the aim and objectives, the scope and limitations, as well as the contribution of the study, will be discussed. Next, Chapter 2 will illustrate the literature reviews on relevant topics that may help in developing the wearable eye tracker. Subsequently, Chapter 3 will go into the methodologies and work plans involved in the development of a wearable eye tracker, such as the hardware setup, gaze detection, the development of a colour detection plugin, and the methods and procedures for performance evaluation. Following this, Chapter 4 will present the results obtained from the performance evaluation and any relevant discussions based on the findings. In addition, several comparisons between the results recorded and previous studies will be carried out. Lastly, Chapter 5 will conclude the study and provide relevant recommendations for future work to potentially improve the prototype.

CHAPTER 2

LITERATURE REVIEW

2.1   Introduction

This chapter will be reviewing other researchers' ideas on the development of wearable eye trackers, including the similarities and differences between researchers' works. Firstly, Section 2.2 will talk about the general working principle for eye trackers. Secondly, available eye-tracking systems around the world will be identified and discussed in Section 2.3. Thirdly, Section 2.4 will discuss the design criteria for wearable eye trackers. Next, mounting platform and hardware setup requirements will be discussed in Section 2.5, while the calibration practices for the eye tracker will be presented in Section 2.6. Section 2.7 will discuss a few applications of eye tracking with computers. Lastly, Section 2.8 will talk about colour detection.

2.2   General Working Principle of Eye Tracker

The earliest eye trackers, they were intrusive and uncomfortable devices for participants (Delabarre, 1898, Huey, 1898). Hence, eye trackers in these modern days are employing the camera-based approach which utilize cameras and infrared light sources, which enable the prevention of visible light interruption. Basically, the eye trackers function by directing near-infrared light towards the centre of user's eyes (pupil), resulting in detectable reflections in the pupil and cornea (the outer-most optical element of the eye). Chugh, et al. (2021) mentioned that multiple infrared light sources can be employed in eye tracking to illuminate the eyes, in which small bright spots named as corneal reflections will be created due to the reflections of IR light at the cornea. These reflections, which is the vector between the cornea and the pupil, are then captured using an infrared camera. For eye tracking glasses, the near-infrared cameras are positioned around the lenses of glasses, either on the frame or directly embedded in the lenses (iMotions, n.d.a).

2.3   Available Eye Tracking System

There are several software tools available for eye tracking, depending on the application and type of eye-tracking system being used. To develop a wearable eye tracker, a head-mounted tracker system is preferable as it provides flexibility to the user. Some of the commonly used software tools for such eye tracking include Tobii Pro Lab, iMotions, and Pupil Labs.

2.3.1   Tobii Pro Lab

This software provides a complete platform for experimenting with eye tracking. Yet, it only offers a few trials without charges. Pouta, Lehtinen and Palonen (2021), Millan, Chaves and Barero (2020), and Best, Boyd and Sen (2023) employed such software in their respective research. It allows users to set up experiments, calibrate eye-tracking systems, and analyse data using a variety of metrics. The synchronization feature in the system enables precise communication on shared events at the start of each stimulus to any compatible biometric device that is simultaneously recording data during the stimulus presentation (Tobii Connect, 2022). To illustrate, Pouta, Lehtinen and Palonen (2021) utilized Tobii Pro Glasses 2 mobile eye tracker with Tobii Pro Lab for the study purpose of the variations in the professional vision of trainee teachers and experienced teachers in natural settings. In addition, the research by Pouta, Lehtinen and Palonen (2021) also aimed to elucidate the relationship between students' immediate attention and the instruction quality of students' knowledge towards the rational number concept.

According to Tobii (2023), near-infrared illumination is used in Tobii Eye Tracking devices to establish reflections on the user's eyes which allow high accuracy of eye tracking. Tobii Pro Lab uses fixation filters to process the information gathered from the input devices. More specifically, the algorithms that built up these filters will compute whether the collected data points belong to the same fixation or not (Tobii, 2022). To illustrate, Tobii Fixation Filter will determine whether the distance between two gaze points is fulling the pre-defined least distance, and Tobii I-VT Filter will determine the two gaze points are whether showing a speed slower than the threshold set (Benjamins, Hessels and Hooge, 2018). As such, when the two gaze points fulfilled one of the criteria of the filters, then the algorithms will define them as the same fixation.

2.3.2 iMotions

This platform incorporates and synchronizes various biosensors attached to the user and provides distinct human insights. It can be used for eye tracking (Kujur, Bhattacharya, Sharma and Kumar, 2022) as well as other physiological measurement tools, such as EEG, ECG and facial expression analysis (iMotions, n.d.b). More specifically, Alvino, Pavone, Abhishta and Robben (2020) mentioned that iMotions can be integrated maximumly of six consumer neuroscience tools, which included facial expression analysis software, galvanic skin response analysis software, eye tracking, ECG and EEG headsets. It provides tools for designing experiments, collecting data, and analysing results. For instance, Kujur, Bhattacharya, Sharma and Kumar (2022) employed iMotions software to evaluate the synchronized data collected from EEG and eye tracker, such as pupil dilation, the relative power of EEG frequency bands etc.

As the visible light spectrum often generate uncontrollable reflections, infrared light is chosen, even though not perceivable by the human eye, to portray the clear separation of the pupil and the iris (Farnsworth, 2022b). The infrared light will enter the pupil directly resulting in visible reflections in the cornea, hence forming a clear and extreme contrast with little noise. This then allows the algorithms to compute the eye movement that leads to the tracking process.

2.3.3 Pupil Labs

This software provides a suite of eye-tracking software tools. The Pupil Core developed by Pupil Labs is an eye-tracking platform that consists of several wearable eye-tracking headsets and an open-source software suite, including Pupil Capture for data collection and Pupil Player for data analysis (Pupil Labs, 2023a). They also share a few design drawings of the hardware needed for the headset. Besides, Pupil Core's API can be used to connect to other devices, which allows customization on the required features by writing a plugin in Python and loading the plugins in the app (Pupil Labs, 2023a), which led to increasing application of such software in eye tracking studies nowadays, such as Niehorster, et al. (2020), Zhao, et al. (2017), and Li, et al., (2018). In addition, Pupil Core is compatible with the iMotions Eye Tracking Glasses Module

(Klaib, et al., 2021). For example, Pupil Labs was utilized by Altvater-Mackensen (2021) to monitor child's attention in natural learning settings. Altvater-Mackensen (2021) built the eye-tracking glasses following the components from the binocular Pupil Labs Core system, which included one scene camera and two eye cameras.

Pupil Labs is employing the same approach as Tobii Pro Lab and iMotions, whereby directing the infrared light to cause the reflection at cornea for the eye movement tracking purpose. There will be two detection pipelines, 2D and 3D pupil detection, running in parallel when the software is being used. The 2D detection will detect the pupil location in the camera image, while the 3D detection will build a 3D model of the eye according to the eye observations to compensate for the slippage issue due to the movement of the eye tracker on the user's face and results in greater accuracy (Pupil Labs, 2023c).

2.4   Design of Wearable Eye Tracker

The design of the prototype must correspond to the application requirements. In this study, design that causes limitations to the head movement should be avoided and so a head-mounted device that is comfortable to the user is more appropriate.

2.4.1   Construction of Prototype using 3D Printer

There are many approaches to 3D printing and each of them implemented different working principles. For example, fused deposition modelling (FDM), inkjet 3D printing, Vat photopolymerization, sheet lamination etc (Lee, et al., 2020, Tumer and Erbil, 2021). Among those approaches, FDM is currently the most budget-friendly and employed method, as it can be operated easily and cheap raw materials are universally available (Sun, Rizvi, Bellehumeur and Gu, 2008, Wickramasinghe, Do and Tran, 2020, Tumer and Erbil, 2021). The 3D printer that operates based on the FDM method will extrude the thermoplastic filaments with precisely controlled temperature and flow rate of the polymer. The object will be printed layer by layer by extruding the fused filaments onto the platform (Tumer and Erbil, 2021). After the fused filaments are extruded onto the build platform, they will cool down, solidifies, and sticks with the adjacent material deposited earlier. The process will continue from layer to layer

until all layers solidify into a final product whose dimensions and shape are pre-determined. Tumer and Erbil (2021) and Mazzanti, Malagutti and Mollica (2019) mentioned that the mechanical strength and surface quality of the printed components are dependent on the polymeric filaments' properties and the printing parameters (i.e., nozzle's temperature, the flow rate of polymer, the thickness of layer to be printed, orientation etc.).

2.4.2   Suitable Materials for 3D Printing

Polymers that are often used in 3D printing with the FDM approach include polylactic acid (PLA), polyamide (PA), polycarbonate (PC), polypropylene (PP), polyethene (PE), and acrylonitrile butadiene styrene (ABS) (Tumer and Erbil, 2021, Parandoush and Lin, 2017). PLA is currently the most utilized raw material for 3D printing with FDM-approach, where it shows a yearly growth rate of ~20 % (Tumer and Erbil, 2021). This may be due to its multicolour appearance with the glossiness and can be printed easily with higher accuracy on the dimensional parts than ABS filaments (Tumer and Erbil, 2021). In addition, PLA is biodegradable and environmental-friendly, which further increased its application in 3D printing (Eynde and Puyvelde, 2017, Wickramasinghe, Do and Tran, 2020). To illustrate, Netco Extruded Plastics (2016) stated the several major applications of PLA, such as medical implants, food packaging, as well as 3D printing.

However, several drawbacks of PLA polymer constrained its application in the fields. More specifically, PLA is less tough, highly brittle, has poor resistance to extensional deformation, poor thermal stability, and narrow processing window (Eynde and Puyvelde, 2017, Wickramasinghe, Do and Tran, 2020). Tumer and Erbil (2021) stated that PLA has weaker mechanical strength than PC and ABS polymers because a more linear molecular chain structure is found in PLA which acts to impart mechanical strength and avoid chain entanglement. Pupil Core Glasses are created using PA12 Nylon instead of PLA and only weighed 22.75 g, which shows greater flexibility as the material for construction (Pupil Labs, 2023d).

Furthermore, PLA is generally thought to be safe for prolonged skin contact as it is biocompatible. Yet, the safety of PLA could change with the alterations in the specific material formulation, the duration and number of skin

contact, and one's sensitivity to PLA (Netco Extruded Plastics, 2016). Allergic reactions, skin irritation, or other serious effects may have occurred on minority when they contact PLA (Netco Extruded Plastics, 2016).

2.4.3 Size and Dimension of Human Head

The head length and head width are important in determining the design of the eye-tracking headset prototype, to ensure the headset can hold in place and be comfortable to the user. Ku, et al. (2020) studied the head dimensions on computed tomography (CT) images and performed direct measurements for the head dimensions. The research showed that the head length is 178.42 ± 6.21 mm, and the head width is 153.20 ± 5.89 mm (Ku, et al., 2020). These results can be used to estimate the length of the supporting arm of the headset and the width of the headset. An average head dimensions data is necessary to ensure the headset is suitable for a variety of people with different head sizes. Besides that, Vasavada, Danaraj and Siegmund (2008) found that the head circumference, head width, head depth, and head height of male subjects are greater than the female subjects. Figure 2.1 shows the lateral and frontal external head and neck anthropometrical measurements, and Table 2.1 illustrates the differences in the head parameters between male and female subjects based on the study from Vasavada, Danaraj and Siegmund (2008).
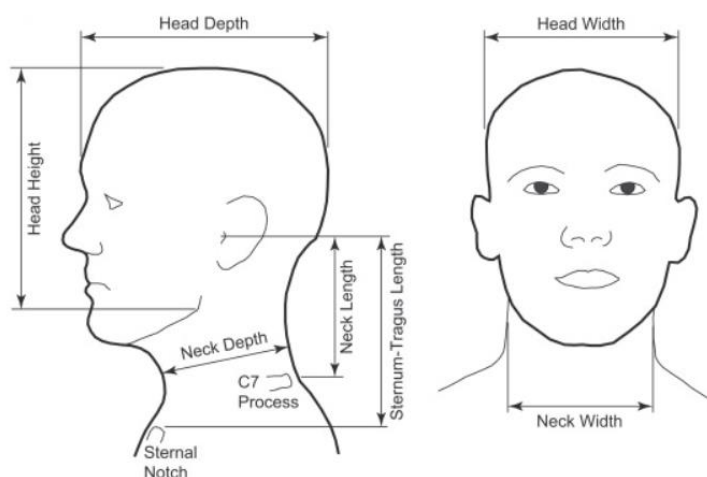
Figure 2.1: Lateral and Frontal External Head and Neck Anthropometrical Measurements (Vasavada, Danaraj and Siegmund, 2008).

Table 2.1:   Mean Head Parameters for The Male and Female Subjects.

Parameter	Male	Female
Head Circumference (mm)	577 ± 13	562 ± 15
Head Width (mm)	153 ± 8	148 ± 8
Head Depth (mm)	199 ± 8	190 ± 6
Head Height (mm)	197 ± 15	184 ± 8

2.5   Mounting Platform and Requirements of Hardware

According to Socha, et al. (2022) and Rantanen, et al. (2011), the general hardware needed for building an eye tracker includes cameras, a specially designed bracket for holding cameras, infrared light emitting diode (LED) as well as the removal of infrared filter in camera. Other than that, four main components need to be included in the prototype design referring to the Pupil Core headset, which includes the world camera, eye camera, nose support, and the cameras mount for each camera. Each headset is usually different in appearance as the camera modules employed are different and it is highly dependent on the design drawings and the availability of the 3D printer in printing complex designs. Figure 2.2 shows one of the Pupil Core headset configurations.

Figure 2.2: One of the Pupil Core Headset Configurations (Pupil Labs, 2023e)

2.5.1   Cameras

There will be one camera employed to capture the view of the user, and at least one camera to capture the eye for gaze tracking. To illustrate, Socha, et al. (2022) utilized three cameras for constructing their wearable eye tracker, in which two cameras were used to capture each eye and one front-facing world camera.

2.5.2   Camera Holder

Besides that, Socha, et al. (2022) designed and 3D printed a few special brackets to secure the cameras in the ideal location and used a regular sunglass as the mounting platform for the gears. The positioning of the cameras and wiring should not affect the visibility of the eyes and should not result in any discomfort when wearing the eye tracker for any application. There will be an extruded compartment on the top of the mounting platform to attach the world camera and a protracted piece on either the left or right side of the frame that acts as an arm extender for the placement of the eye camera near the designated eye. Figure 2.3 shows a complete prototype of a wearable eye tracker.
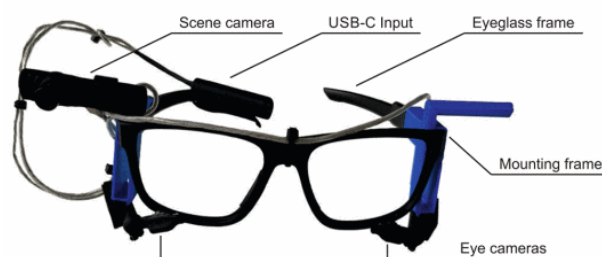
Figure 2.3: Wearable Eye Tracker Prototype (Socha, et al., 2022)

Figure 2.4: Visualization of Pupil Pro Eye Tracking Headset on User
               (Schindler, et al., 2016).

2.5.3   Infrared LED

Infrared (IR) light source is one of the essential elements for the development of wearable eye trackers. Infrared radiation can be found naturally from solar radiation and fire. There are also a few artificial infrared radiation sources,

which include heated metals, molten glass, plasma torches etc (Clflores, 2018). To obtain clear corneal reflection, the IR source has to position adequately close to the eye camera as well as the user's eye, and the active IR light source will produce bright/dark pupil images. The bright/dark pupil effect can be distinguished properly when using more than one IR light source, which then allows the detection of the pupil after thresholding the differences in the images (Zhu and Ji, 2005). Examples of infrared LED include TSAL6100, VSMB2943GX01, VSMY1850X01, and SFH 4050-Z.

The most fundamental IR source can be created using the IR LEDs with appropriate circuitry designs. Generally, the forward voltage of such LED is ranging from 1.2 V to 3.4 V, depending on the colour and model of the IR LED. For instance, TSAL6100, an IR LED, has a forward voltage of 1.35 V when tested with 100 mA for 20 ms (Vishay, 2014). The component of IR LED is sensitive to overheating, and thus it burns out easily when a forward voltage that is higher than as stated in the data sheets passed through.

Besides that, safety exposure of the infrared light to the user must be contemplated properly in the design considerations. According to World Health Organization (WHO), the biological impacts due to IR exposure are highly dependent on wavelength and exposure time, in which unacceptable effects occur only when specific threshold intensities are surpassed. Since the infrared light is not visible to the human eye, it is impractical to depend on subjective justifications from the user regarding the brightness of IR LED to identify whether the IR irradiance exceeds the safety threshold. In 1994, the American Conference of Governmental Industrial Hygienists (ACGIH) and other international organizations, including WHO, suggested and published the threshold limit values which aim to minimize any delayed effects on the eye's lens as well as heat harm to the retina and cornea. The delayed effects due to infrared radiation are possibly causing the formation of cataracts (Clflores, 2018). Therefore, the infrared radiation at wavelengths between 770 nm to 1400 nm should be restricted to 100 W/m^2, based on a pupil diameter of 7 mm, to prevent potential delayed effects on the eye lens and overexposure at the cornea (Matthes, 2011, Clflores, 2018). Additionally, the camera could perform adequately in detecting the gaze information with a source that has an irradiance level below 100 W/m^2. Hence, it is safe to employ the IR LED or a surface-

mounted IR source near the user's eye, as it is in an acceptable safety level below 100 W/m^2.

2.5.4   Infrared Filter

Most of the camera module is originally equipped with an infrared filter, which is also known as a hot mirror (Adams, Parulski and Spaulding, 1998). The main purpose of the IR filter is to block out the infrared light from the camera's sensor. In other words, the hot mirror reflects infrared energy as it is a type of heat energy and enables the transmission of any light under its cut-off wavelength ranging from 600 nm to 700 nm. An IR filter will be placed in front of the camera lens to block out the light that is within the range of infrared wavelength (780 nm to 1 mm). Such wavelengths are above the red visible light, and hence they are not visible to human eyes. Without the IR filter, the camera would capture both visible and infrared light, which results in distorted colours and images. In addition, the infrared light that is not filtered out will interfere with autofocus and cause blurring in images.

2.5.5   Nose Support

Nose support is also important when designing the prototype to ensure the comfort of the user and to enhance the stability of the headset on the user's head. Based on the available designs of spectacles frames, the nose support for the headset can be designed with or without silicon nose pads, which is similar to some of the existing frame designs. Hence, a properly designed nose support could reduce the slippage issue for more accurate gaze detection. Figure 2.5 shows the nose support of a Pupil Core headset that is equipped with a silicon nose pad.

Figure 2.5: Pupil Core Headset with Nose Support Equipped with a Silicon
Nose Pad (Pupil Labs, 2023e).

2.6 Calibration for Eye Tracker

According to Gwizdka, Zhang and Dillon (2019), about 50 to 70 cm is the common distance where the user has to be seated from the screen during calibration, but still depending on the respective model. The user will be asked to stare at a specific location in the surroundings or a moving dot on the screen throughout the calibration process. The presentation of markers is referred to as choreography, and there are several choreographies provided by Pupil Core. Examples of choreographies include screen marker calibration choreography, calibration marker, single marker calibration choreography, and natural features calibration choreography.

Screen marker calibration choreography and calibration marker are selected to be reviewed and discussed accordingly. Firstly, screen marker calibration choreography is the default choreography, which displays the markers on the screen. The user's eye has to follow the markers presented with the least head movement during the process. Additionally, the marker size and sample duration can be altered to suit the user's calibration to ensure optimal results. Secondly, Pupil's Circular Calibration Marker can be downloaded from the website to serve as another calibration choreography. Pupil Capture can detect the markers automatically in the world video. Pupil Calibration Markers are used in calibrating the eye tracker while showing the Stop Marker can then finish the calibration process. Figure 2.6 illustrates the calibration markers downloaded from Pupil Labs.
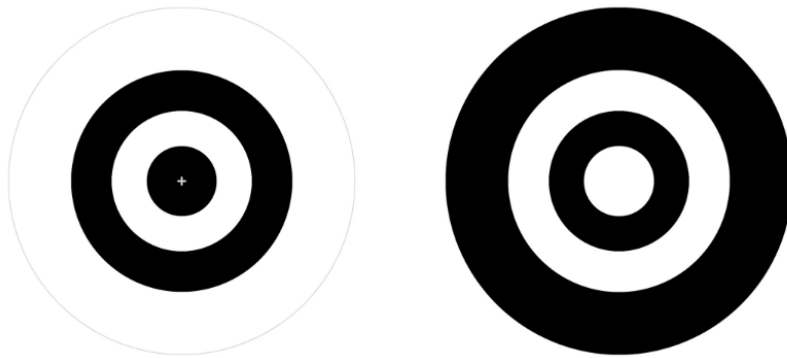
Figure 2.6: Pupil Calibration Marker (Left) and Stop Marker (Right) (Pupil Labs, 2023c).

2.7   Application of Eye Tracking with Computer

With the development of blink detection and dwell duration in the eye tracker, the user is allowed to control the cursor more precisely and accurately for purposes such as scrolling or clicking. By detecting blinks, the eye-tracking software can determine when the user wants to perform an action (e.g., clicking or scrolling), and carry out that action accordingly. For example, if the user wants to click on a button or link, it can be done easily by the user by blinking their eye twice quickly which can be detected and recognized as a click command.

Based on studies, integration of blink detection and dwell time for the interaction with a computer is important for users that have motor impairments or disabilities. This integration allows them to control the cursor and interact with computers more easily and efficiently. According to Microsoft (n.d.), Microsoft has developed eye control as one of the interaction approaches in Windows. However, the current eye control system only supports eye trackers which are primarily from Tobii devices. Hence, eye control applications that work with other software have recently focused on benefiting individuals who use a do-it-yourself approach in developing their own wearable eye tracker.

2.7.1   Blink Detection

The confidence level will be computed during the data collection by assessing the accuracy of pupil detection for a particular eye picture. It is ranging from 0.0 to 1.0, depending on the quality of pupil detection. If the pupil could not be

detected, it would be 0.0. Meanwhile, 1.0 is the highest possible level, in which the detected pupil is with very great assurance.

There is a Blink Detection plugin in the Pupil Capture that serves the purpose of capturing the eyeblinks. It makes use of the fact that during a blink, the closing of the eyelid would cover the pupil causing the computed 2D pupil confidence to decrease rapidly, followed by a swift increase in confidence level when the pupil can be captured again. The 2D pupil confidence values will be convolved before processing using a filter implemented in the blink detector. The filter response would surge more abruptly when confidence drops occur, and vice versa when confidence level rises.

In the software, the threshold for both the onset and offset confidence as well as a filter duration in seconds can be adjusted accordingly to obtain optimal blink detection. Firstly, the onset confidence threshold is to categorize the onset of blinking when the filter response is greater than the threshold, parallel with a rapid decline in the pupil confidence level. Secondly, the end of a blink is categorized by offset confidence threshold, where the pupil confidence would increase correspondingly. Lastly, filter length is the duration for the detector to identify the changes in confidence level.

With high-quality eye data with reliable pupil recognition, the blink detector's default settings appear to function quite satisfactorily. Yet, it is still necessary to modify the threshold in the case where blinks are not correctly identified. Hence, it is crucial to comprehend the types of errors that might happen and be able to recognise them when they occur, so that appropriate corrective actions can be taken. Table 2.2 briefs the three common errors that would occur during blink detection based on Pupil Labs. Other than that, poor pupil detection would also result in false negatives for blink detection. Although the blinks can be more easily detected by adjusting the thresholds, the possibility of false positives would also rise accordingly. Therefore, it is worth spending time in positioning the eye camera and setting the 2D pupil detector to ensure an optimal setup so that more accurate results can be obtained.

Table 2.2:   Type of Errors That May Occur in Blink Detection.

Type of Error	Description	Cause
False negatives	Blinks are not detected	Too high onset threshold
False positives	Blinks detected even though there is no blink	Too low onset threshold
Erroneous blinks with irrational durations	End of blink is not detected	Too high offset threshold

2.7.2   Mouse-Clicking

Clicking is one of the common actions when interacting with the computer. It can be achieved through the combination of blink detection and dwell time in eye tracking technology. Dwell duration describes the amount of time the user's gaze remains fixed on a specific location, which can be detected by the eye tracker.

The user can first focus their gaze on the desired area on the screen, such as a button or link, to initiate an eye-tracking click. The click command is initiated when the user blinks his or her eye, which is detected by the eye tracking software as a click signal. The dwell duration can also be integrated into the eye control application as a supplementary command input to ensure accurate and reliable clicking. For instance, the software may require the user to maintain their gaze on the target location for a pre-determined duration, such as two seconds, before the click instruction is carried out. This could potentially prevent any unintentional clicks from the user and reduce false positives due to erroneous blinks (McCurley and Nathan-Roberts, 2021).

2.7.3   Web Pages or Applications Scrolling

Scrolling can also be achieved similarly to clicking, which employs the combination of blink detection and dwell duration in the eye tracking software (Shah, 2020). Figure 2.7 illustrates the indicated regions and scroll bar in the webpages or applications.
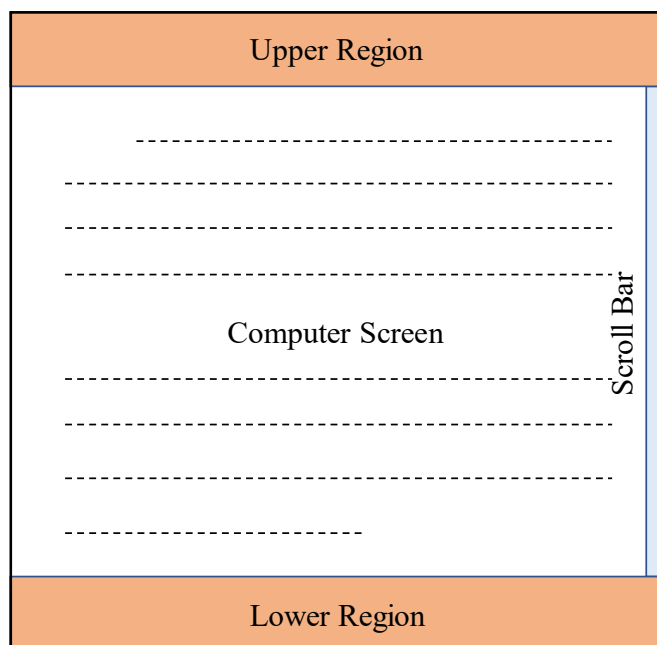
Figure 2.7: Visualisation of Webpages or Applications with the Scroll Bar and
Indicated Upper and Lower Regions.

To initiate scrolling, the user's gaze can be first directed to the scroll bar which is generally available on webpages or applications. Next, the clicking function is performed by the user through an eye blink to move the scroll bar in the desired direction. Other than blink detection, the user's eyesight can also be utilized to perform scrolling. As visualized in Figure 2.7, there will be two regions, named "Upper Region" and "Lower Region". When the user's eyesight is detected for staying more than 3 seconds in either region, the respective scrolling activity will be carried out. For example, the scroll upwards operation will be executed when the user's eyesight moves into the Upper Region and stays for 3 seconds, and vice versa for the scroll downwards action. In other words, scrolling is not performed whenever the user's eyesight falls between the Upper and Lower regions, while scrolling occurs whenever the user's gaze is directed into either region. As a result, both the manual and unintentional scrolling of the screen can be possibly avoided.

Moreover, dwell duration can also be applied in scrolling to adjust the scrolling speed. For instance, if the user's gaze remains in either region for a brief period, such as 5 seconds, the software will interpret this as a signal to slightly increase the scrolling speed.

2.8 Colour Detection

There are various applications being developed to help the visually impaired and blind individuals in identifying the objects' colour in real life. Particularly, colour detection is one of the major applications that ease their life. In the study carried out by (Nasir, et al., 2021), a deep learning approach was involved to develop an Android-based application for the visually impaired. The phone camera will be used to capture the object, and the colour name will be analysed based on the Red-Green-Blue (RGB) values of the detected image. Besides, Al-Doweesh, Al-Hamed and Al-Khalifa (2014), an application that used a smartphone's camera to capture image data for data processing. The colour detection was then done using Hue, Saturation, and Lightness (HSL) colour space, instead of RGB colour space. This is because the RGB channels interfere with each other and their chrominance and luminance are mixed, accordingly, a small variation in lighting will affect the rates for the red, green and blue components (Le, et al., 2010; Al-Doweesh, Al-Hamed and Al-Khalifa, 2014).

2.9 Summary

In short, corneal reflection is employed in most of the recent eye-tracking software, such as Tobii Pro Lab, iMotions, and Pupil Labs. Pupil Labs has been increasingly utilized in gaze-related studies as it is open-source software and is highly customizable for further integration. Besides, some studies showed that the eye tracker can be constructed using 3D printing and PLA filaments, which is biodegradable and environmentally friendly, to customize the mounting platform that suits different head size. Moreover, calibration is essential before performing gaze detection to obtain accurate and reliable results. As there are many choreographies available for calibration, selecting the best calibration choreography can ease the process and help in producing optimal gaze detection results. With the development of technology, eye trackers can now easily be employed in computer applications to allow the interaction between user and computer. Examples of applications include blink detection, mouse-clicking, and web pages or application scrolling. Colour detection is important and useful for individuals with colour blindness, which can be established by collecting the RGB or HSL values using camera.

CHAPTER 3

METHODOLOGY AND WORK PLAN

3.1 Introduction

This chapter will discuss the methods employed to develop an affordable, wearable eye tracker. Section 3.2 presents the overall flow of the approaches employed in the project. Next, Section 3.3 will discuss the hardware setup, which involves the modification of the camera module, fabrication of the mounting platform, construction of infrared LEDs onto the camera module, and the removal of the infrared filter. Moreover, Section 3.4 will talk about gaze detection using the constructed hardware. Both the hardware and software settings as well as data collection will be included in this section. Next, Section 3.5 will discuss the development of the colour detection plugin which can be used in Pupil Capture. Lastly, Section 3.6 will talk about the methods employed in evaluating the performance of the developed wearable eye tracker.

3.2 Preliminary Planning and Conceptual Design

Generally, the development of a wearable eye tracker is separated into two major phases, which are the hardware setup and gaze detection using the software. Hardware or tools that were utilized in this project include camera module "GENERAL WEBCAM" (30 mm × 25 mm) and "USB Composite Device" (30 mm × 25 mm), infrared LEDs (VSMB2943GX01), a 3D printer, a laptop, and tiny screw and nuts. Meanwhile, SOLIDWORKS was used to design the mounting platform for the prototype and Pupil Labs, especially Pupil Capture, was employed as the eye-tracking software in this project. Figure 3.1 illustrates the flowchart which summarises the workflow of this project.
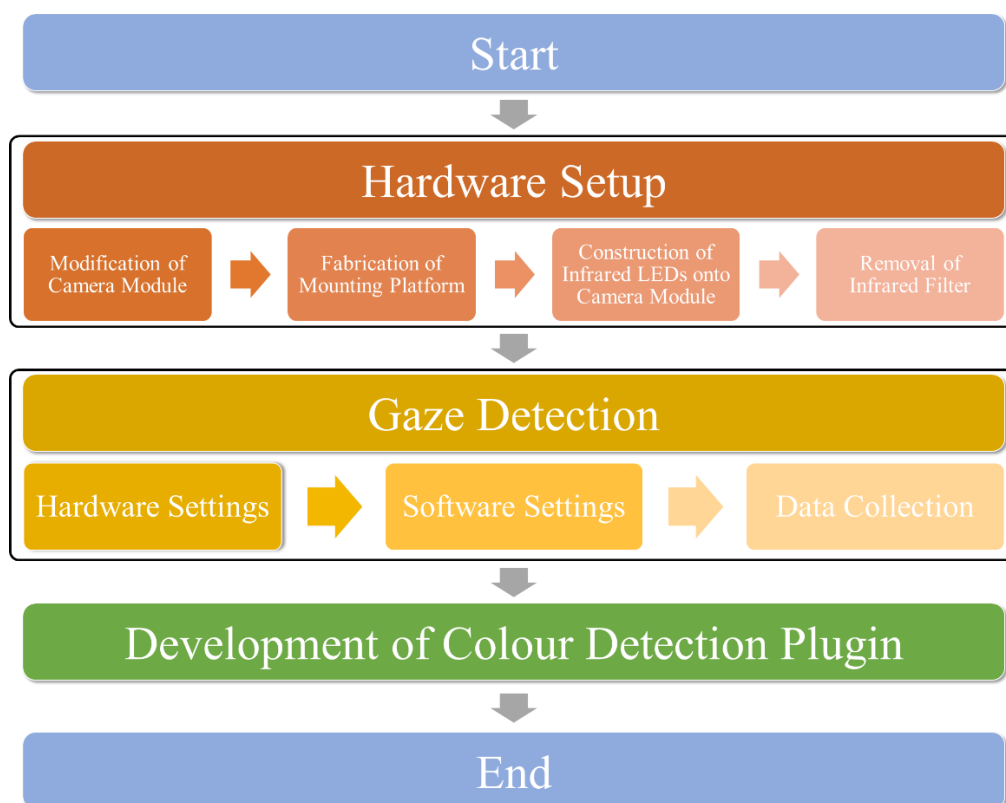
Figure 3.1: Flowchart of Summarized Workflow for The Project.

3.3 Hardware Setup

3.3.1 Modification of the Camera Module

The camera modules employed in this project was obtained from web cameras and a monocular eye-tracking setup were used to construct the prototype. In other words, two cameras were employed, in which one served as the world camera and another as the eye camera. Although one eye camera could show relatively poor accuracy than two eye cameras, one eye camera was adequate as it was still applicable for gaze detection and possibly reduced the overall weight of the prototype. To reduce the weight and size of the prototype, the casing of the web cameras was disassembled carefully without damaging the camera modules. It is important to ensure that the camera modules can support the desired resolution and frame rate. More specifically, the selected camera modules in this project can support at least a resolution of 1280×720 and a frame rate of 30 fps to ensure a clear video captured by the camera without any significant delay in the frame that may affect the detection. Figure 3.2 shows the camera module disassembled from the web camera.
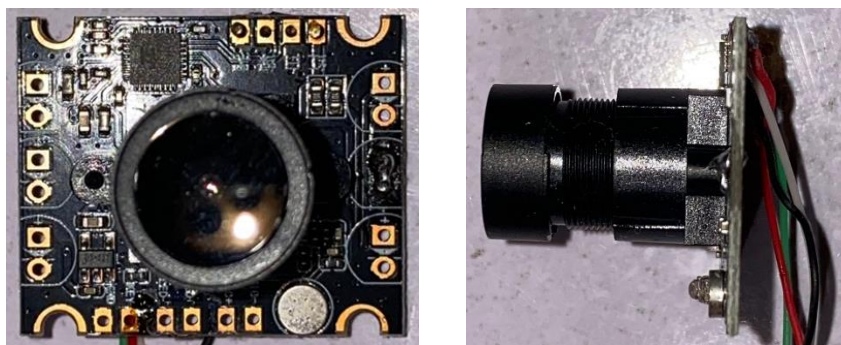
Figure 3.2: Front View (Left) and Side View (Right) of The Camera Module
Disassembled from The Web Camera.

3.3.2   Fabrication of the Mounting Platforms

The frame was designed to fit most head sizes and exhibit enough strength to support other components (e.g., world camera and eye camera) as well as be satisfying for extended usage without obstructing the user's vision. An adjustable extended arm that connects to a rotatable (in a single plane) camera mount for the eye camera will be constructed for the prototype so that the eye camera can be optimally positioned based on different head sizes for proper eye fitting.

On the platform where the community is collaborating and sharing their experiences, it can be found that many individuals are using the do-it-yourself approach to develop an eye tracker that operates using Pupil Capture software. Some of the design drawings available on that platform were referred to during the design process, and the drawings will be modified according to the components employed, especially the camera holders that were used to hold cameras, which are different in shape and size. Examples of the available designs include the world camera holder, extender arm with ball joint, and screw.

To create the mounting platform for the eye tracker, SolidWorks was first used to construct the design drawing for the mounting platform. As reviewed, nose support is important to ensure comfortability and stability of the headset, hence it was included as part of the design. 3D printing was then employed to create the customized prototype components, and PLA filament was used for performing such printing in the laboratory after considering its risk-benefit factors (i.e., ease-of-use and dimensional accuracy) and the cost. Figure 3.3 presented the available world-camera drawing using SolidWorks on

the platform and Figure 3.4 showed the 3D printed world-camera holder from the available drawing.
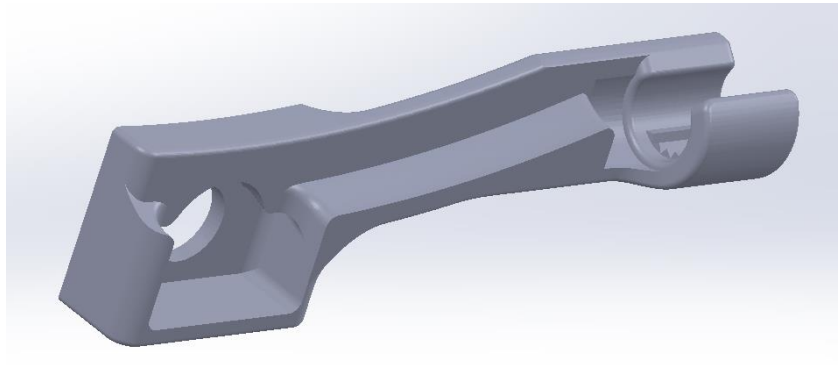
Figure 3.3: Available SolidWorks Drawing for World-Camera Holder.

Figure 3.4: 3D Printed World-Camera Holder.

The initial design for the mounting platforms was designed as a unified one-piece structure, encompassing all mounts except for the eye-camera mount, which remained separate from the frame. Figure 3.5 illustrates the preliminary design for the mounting platform.
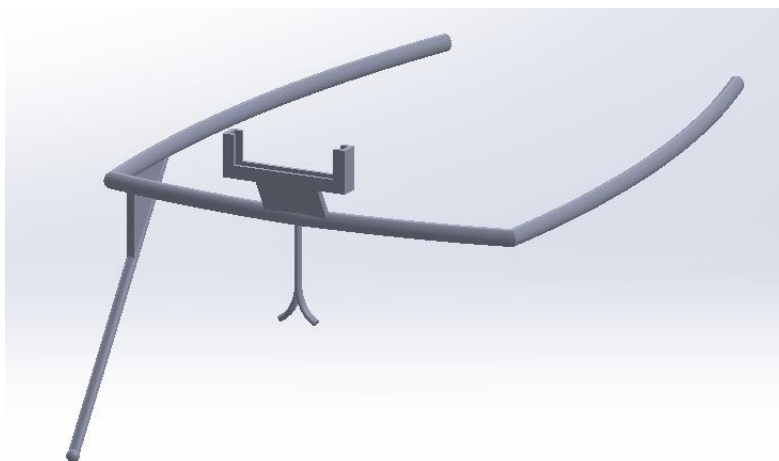
Figure 3.5: Preliminary Design Drawing for Mounting Platform.

However, ball-joint design was not achievable using the PLA-printed structures as they were hard and not flexible, which prevented them from being tightened as intended. Hence, it was replaced with a simple hinge joint design, whereby only single-plane rotation is available. Moreover, the design was improvised into several detachable mounting structures that can be attached to a readily available plastic frame. The detachable mounting structures included the eye-camera mount, world-camera mount, hinge arm, extender arm, and hinge base for the world camera. These detachable designs provide convenience to the user by keeping the eye tracker in a small container when transporting it from one place to another. Additionally, these designs allow the user to replace each broken structure individually, which reduces the burden of replacing the entire mounting platform, which is relatively costly.

3.3.3   Construction of Infrared LEDs onto Camera Module

To obtain clear corneal reflection, the small infrared LEDs have to be positioned adequately close to the eye camera as well as the user's eye to create bright/dark pupil images. The surface-mount IR light source will be soldered onto the board of the "USB Composite Device" camera module on the designated pins. The soldering temperature will be maintained below 260 °C as it is the maximum soldering temperature based on the datasheet. It is important to identify the cathode and anode of the IR LED before soldering it onto the camera module. This can be done by referring to the VSMB2943GX01's datasheet. To aid the soldering process, solder flux will be used to possibly remove oxides and

enhance the flow of solder onto the circuit board of the camera module. Figure 3.6 shows the IR LED soldered onto the designated LED pin on the board of the camera module.
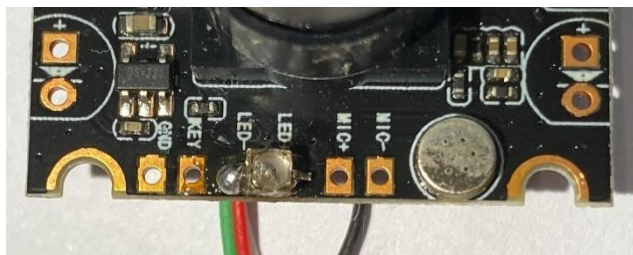
Figure 3.6: Camera Module with Soldered IR LED.

3.3.4 Removal of the Infrared Filter

As the corneal reflection is employed for eye tracking, the IR filter has to be removed to ensure the eye camera can capture the reflection caused by the infrared light. Yet, removing the IR filter is a complex process, which requires specialized tools and technical skills, and it can damage the camera if not done correctly. Therefore, the camera module employed in this project will be first tested on its capability to capturing infrared light using an external IR source. If the infrared lights are able to be captured using the camera module, corneal reflection is possible to be captured by the eye camera, and hence the complex process of removing the IR filter can be ignored. If the IR light is filtered, then the filter will be to be removed and replaced with an exposed film. In this study, the IR filter will be removed and replaced with exposed film. Figure 3.7 shows the IR filter equipped on the lens of the camera module, while Figure 3.8 presents the replacement of the IR filter with exposed film.

Figure 3.7: IR filter in the Lens of Camera Module.

Figure 3.8: Replacement of IR Filter with Exposed Film.

3.4 Gaze Detection

The selection of eye-tracking software depends on the specific requirements of the application, the available hardware, and the expertise of the user since each software tool has its advantages and disadvantages. After considering the available software for eye tracking, Pupil Labs was selected as the software tool for this project. This is mainly because it is open-source, highly customizable, and allows further integration with other instruments, such as wheelchairs, even though requires some advanced skills in the design and programs. In addition, Pupil Labs software includes Pupil Capture, Pupil Service, Pupil Player and other applications, which provide many integration opportunities for the user.

The procedure for performing gaze detection was characterized into three main phases, which are the hardware settings, software settings, and data collection. Each of the phases will be discussed in detail in the following parts.

3.4.1 Hardware Settings

3.4.1.1 Laptop Setup

The laptop being utilized in this project is the ROG Strix G531GT. This laptop is equipped with Intel® Core™ i5-9300H CPU at 2.40 GHz and 8 GB RAM while operating in Windows 11. To ensure the stability of the software, proper power supply as well as sufficient processing power and memory will be verified before connecting the eye tracker, so that the device can handle the eye tracking data collected to generate the visualizations and perform any analysis when required.

The eye tracker will be connected to the laptop that is equipped with Pupil Capture software through a USB connection. There will be a common issue when connecting those non-Pupil Labs hardware with the software, since

the drivers of the hardware, such as camera modules, have incompatible USB drivers that suit the software. As a result, the Pupil Capture programme would not be able to recognise the camera attached to the device. This issue can be resolved easily by using Zadig. It is a driver modification software, which can replace the driver of the device with the desired one. Firstly, the compatible driver named 'libusbk 3.0.7.0' was downloaded to the computer for replacement later. After starting Zadig, all devices available were listed in the software. The connected camera module was selected, and its driver was changed from WinUSB to libusbk 3.0.7.0. By completing the above steps, the camera module was detected by Pupil Capture software and was employed as the image source.

3.4.1.2   Mounting Headset Adjustments

All the cameras will be attached securely to the 3D printed headset, and the headset will then be stably placed onto the user's head. More specifically, the nose support will be in a comfortable spot for the user to safeguard a good user experience while ensuring the headset remains in place during data collection. Since the head size varies between users, necessary adjustments on the headset will be executed to properly fit the user's head.

3.4.2   Software Settings

3.4.2.1   Fine-Tuning for Pupil Detection

In the Pupil Capture, both the 2D and 3D pupil detection pipelines are running in parallel when started. It is essential to make some adjustments in the 2D pupil detector to enhance the detection of pupils. To make such adjustments, the eye window will be first changed to Algorithm Mode view, followed by using the Pupil Detector 2D plugin that allows the setting for maximum and minimum pupil size as well as the intensity range.

There will be two red circles and one green circle in the Algorithm Mode. The two red circles represent the maximum and minimum size of the pupil, while the current pupil size in the captured frame will be shown as a green circle. Hence, the maximum and minimum values for pupil size settings will be adjusted appropriately to ensure that the current pupil size (green circle) always falls within the set range for all eye movements.

The lowest "darkness" of a pixel that can be categorized as the pupil can be regulated through the intensity range. The pixels detected as parts of the pupil will be presented as blue in the mode. Therefore, the intensity range will be corrected to a certain where the pupil is fully covered with the least leakage outside the pupil.

In addition, the modelled eyeball will be surrounded by a steady circle for a well-fit 3D eye model, whereby the circle is correspondently sized to the respective eyeball. The colour of the circle varies depending on the physiological bounds' status. If the model has a dark blue steady circle, it means that the model is inside physiological boundaries, where this is the ideal condition; if it has a light blue circle, it is outside of physiological constraints. Thus, the fitting will be adjusted accordingly to achieve the optimal fitting condition that allows reliable detection. Figure 3.9 shows the colour changes of the circle in eye model fitting.
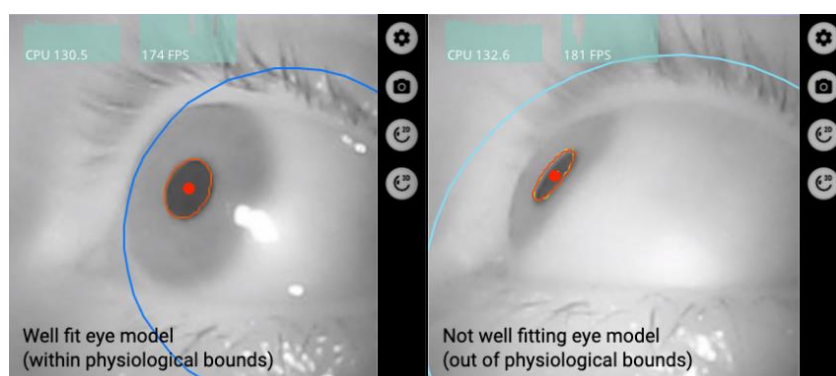
Figure 3.9: Eye Model Fitting Status with the Colour Changes of Circle (Pupil Labs, 2023f).

3.4.2.2 Calibration

There will be a world camera to record the user's field of vision and one eye camera to record the user's gaze movement. Hence, calibrations will always be required before starting actual data collection for visualization. It is necessary to make sure that the user's pupil is accurately identified and monitored before starting the calibration process. In addition, the whole region that is to be calibrated will be adjusted so that it is visible inside the world camera's field of view (FOV) and the world camera is focusing on the designated distance.

Screen marker calibration choreography will be employed in this project as a calibration approach for the eye tracker. Firstly, the user will be seated about 50 to 70 cm away from the screen with the headset placed on the head. In Pupil Capture, the user will be asked to press C on the keyboard or the C button on the left side of the world window to start the calibration after one is ready. Figure 3.10 shows the C button in the world window.
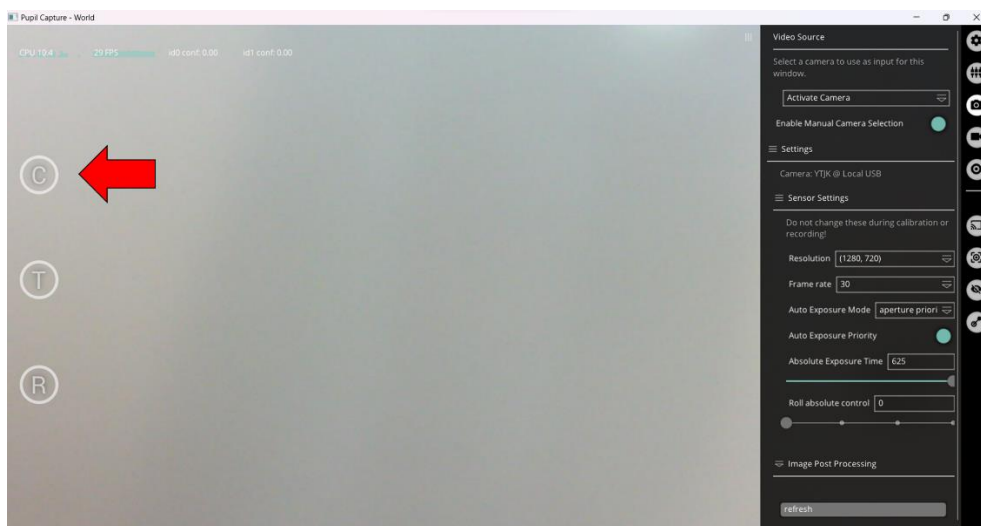
Figure 3.10: C Button in the World Window.

After starting the calibration, the user will be instructed to stare at a moving dot on the screen throughout the calibration process. The user will be reminded to follow the markers presented on the screen with the least head movement during the process. In addition, the marker size and sample duration will be altered to suit the user's calibration to ensure optimal results. The calibration window will be closed automatically once the calibration is completed. Figure 3.11 shows a similar calibration marker presented on the screen.

Figure 3.11: Pupil Screen Calibration Marker (Pupil Labs, 2023c).

3.4.2.3 Data Processing on Calibrated Data

Real-time data processing of the collected gaze data will be performed in parallel with the calibration to allow instant visualization of the world camera view. The calibration data will be collected for the purpose of linking the eye camera to the world camera. More specifically, the calibration data will be employed to refine the eye tracking system to ensure reliable measurements, which creates a mapping function that relates the raw gaze data to screen coordinates and applies to the data collected during the subsequent data collection stage. Real-time data processing will be more limited, whereby only basic filtering and feature extraction will be performed automatically by the software.

3.4.2.4 Data Analysis and Interpretation on Calibrated Data

Accuracy of gaze detection is one of the crucial factors for the success of eye trackers. Hence, the Accuracy Visualizer plugin provided by the software will be employed to identify the accuracy and precision of the performed calibration. The mean angular offset, which is measured in degrees of visual angle, between fixation sites and the corresponding positions of the fixation targets serves as the basis for accuracy calculations. By utilizing the plugin, the discrepancy between the recorded matching gaze locations and the reference points will be presented. Based on Pupil Labs, the user will be able to accomplish an accuracy ranging from 1.5 to 2.5 degrees when utilizing the 3D pupil detection pipeline. In addition, the calibrations would only be accurate inside the calibrated field of vision in the world camera. To illustrate, poor accuracy will be found in the left

half if the user solely focuses on the markers that are on the right half during the calibration process.

3.4.3 Data Collection

After calibrating the eye tracker, the user will proceed to the eye tracking application. Pupil Capture will provide real-time visualization of the eye movements in a small window and show the view captured from the world camera in the world window. The eye camera will be examined throughout the data collection stage to ensure the pupil is detected all the time to produce accurate and reliable results. During the real-time data collection, the user will be instructed to perform several tasks. The eye movements corresponding to the view location on the text will be recorded using Pupil Capture software. In addition, the gaze data (e.g., confidence level, gaze duration etc.) will be recorded and processed for further application.

3.5 Development of Colour Detection Plugin

A colour detector plugin was developed using Python and the fixation detector plugin is readily in Pupil Capture as reference. This approach significantly could shorten the workload needed in developing the intended plugin and ensure that the variables in the written code synchronised with the source code.

3.5.1 Colour Detection using RGB Values (Version 1)

The three main colours that make up every colour are red, green, and blue. Each colour value is represented by a number between 0 and 255. Hence, there are about 16.5 million combinations for expressing a colour. The world camera for the eye tracker will capture the pixel RGB values after the fixation is detected. Subsequently, the RGB values will be displayed at the top left of the world view window.

3.5.2 Colour Detection using HSL Values (Version 2)

As hue, saturation, and lightness are three distinct components in HSL colour space, HSL colour space was utilised in developing the colour detection plugin in Pupil Capture. Hues, often referred to as colours, are determined by the wavelength of reflected light; saturation refers to the intensity or purity of a

given colour, with increased saturation resulting in a brighter appearance and decreased saturation leading to a duller appearance; lightness describes the extent to which black or white is mixed with a chosen hue, with the colour appearing lighter when white is added and darker when black is added (Bradley, 2013).

The pixel RGB values recorded by the world camera will first be converted to HSL, followed by the colour name analysis. The values of hue, saturation, and lightness will be used to detect the colour based on the pre-classified colours' categories. Classification of hue, saturation, and lightness values was performed with reference to Al-Doweesh, Al-Hamed and Al-Khalifa (2014). Table 3.1 illustrates the colour categories relating to saturation and lightness values, while Table 3.2 shows the colour categories corresponding to hue values.

Table 3.1: Colour Categorisation Relating to Saturation, and Lightness.

Colour Name	Criteria of Saturation (S) and Lightness (L)
White	$L > 90$
Black	$S \leq 15$ and $L \leq 15$, or $L < 10$
Dark Grey	$S < 16$ and $L \leq 40$
Grey	$S < 16$ and $L \leq 70$
Silver	$S < 16$ and $L \leq 80$
Light Grey	$S < 16$ and $L \leq 95$

Table 3.2: Colour Categories Corresponding to Hue Values.

Colour Name	Criteria of Hue (H)
Red	$0 \leq H \leq 15$, or $346 \leq H \leq 360$
Orange	$16 \leq H \leq 40$
Gold	$41 \leq H \leq 45$
Yellow	$46 \leq H \leq 60$
Yellow-Green	$61 \leq H \leq 90$
Green	$91 \leq H \leq 135$
Spring Green	$136 \leq H \leq 160$

Cyan	$161 \leq H \leq 200$
Blue	$201 \leq H \leq 255$
Purple	$256 \leq H \leq 300$
Pink	$301 \leq H \leq 345$

During the analysis, saturation and lightness will be first examined to detect "black", "white", and "grey" colours. If none of these colours are detected, the search will be proceeded by using the recorded hue value with the predefined hue range. As the possibility of achieving the exact HSL value is relatively low due to the quality of the camera sensor or the environment lighting, the difference between the recorded HSL value from the world camera and the pre-classified HSL colour values within the category will be computed. This approach is to identify the nearest value, and hence the detected colour will be classified under that particular colour with the nearest value. Subsequently, the name of the detected colour will be displayed at the top left colour of the screen in the world window.

3.6   Performance Evaluation Method and Procedure

3.6.1   Angular Accuracy, Angular Precision, and Data Loss

3.6.1.1 Pre-Test Setup

A total of five participants were recruited to be involved in the testing of the developed prototype. The test will be carried out in a fluorescent tube-lit room, and the participants will be seated 0.5 m away from the computer screen where the entire screen is visible in the world camera. Additionally, the brightness of the computer screen was fixed throughout the testing for all the participants to ensure the reliability of the results. Each time a participant donned each of the head-worn eye-tracking setups, the operator first inspected the eye camera video stream and made adjustments as necessary to guarantee that the eye was clearly visible. The developed headset was set up by adjusting both the eye camera orientation and focus. The operator then inspected the world camera image and instructed the participant to adjust their head pose if required to make sure that the complete computer screen was visible.

Next, the operator checked on the eye model fitting status, whereby the fitting will be altered to accomplish the optimal fitting condition shown by a dark blue circle that allows reliable detection. Calibration was then performed using the calibration plugin in the Pupil Capture, where the on-screen markers appeared in a fixed position on the screen. The quality of calibration was then examined by performing validation, where the on-screen markers appeared in random positions on the screen. The size of the markers was fixed to 2.0 throughout the entire testing procedure. The calibration will be performed again if there is any reported gaze data significantly outside the validation markers.

3.6.1.2   Test Procedure

Once the calibration was completed, the participants were instructed to perform a series of designed tasks to evaluate the performance of the developed prototype. There will be a total of seven tasks for each participant, and each task requires three repetitions to obtain the average of recorded values. The mean and standard deviation can be computed based on Equation 3.1 and Equation 3.2, respectively.

$$Mean, \bar{x} = \frac{Sum\ of\ Observations}{Total\ Number\ of\ Observations} \qquad (3.1)$$

$$Standard\ Deviation, \sigma = \sqrt{\frac{\sum(Value\ Observed - Mean)^2}{Total\ Number\ of\ Observations}} \qquad (3.2)$$

All the tasks were designed by referring to Niehorster, et al. (2020) and Chan (2021). Tasks (1) and (2) aim to evaluate the performance of the eye tracker in a non-movement condition. Task (3) and (4) serve to assess the eye tracker's performance during facial movement and expression, while Task (5), (6), and (7) serve to examine its performance during head and eye tracker movements. For each of the seven recordings per participant, gaze data were recorded for the following seven conditions in the following sequence. Table 3.3 displayed the description for respective tasks.

Table 3.3: Descriptions of Task (1) to (7).

No.	Task	Description
1	Calibration	Participants will be instructed to fixate at the centre of the on-screen calibration markers throughout the calibration process, keeping their heads still until calibration is completed.
2	No Movement	Participants will be instructed to fixate at the centre of on-screen calibration markers for 7 seconds. Sample duration can be adjusted in the screen marker calibration settings.
3	Speech	To demonstrate the hardware movement and slippage issue during speech, participants will be instructed to recite the alphabet from A to Z while fixating the on-screen calibration markers.
4	Facial Expression	To assess potential hardware movement and slippage induce by facial expressions, participants will be instructed to repeatedly raise their eyebrows for 10 seconds at a rate of ~1 Hz (raising every second) while fixating the on-screen calibration markers.
5	Horizontal Head Movement	To simulate potential head movement-induced slippage, participants will be instructed to perform continuous horizontal head rotations (left to right and right to left) at frequency of ~1 Hz for 10 seconds while fixating the calibration markers.
6	Vertical Head Movement	The conditions mimicking horizontal head movement will be replicated, with participants instructed to perform repetitive vertical head movement (top to bottom and bottom to top).
7	Depth Head Movement	The conditions mimicking horizontal head movement will be replicated, with participants instructed to perform cyclic depth head movement (towards and away from the screen).

Moreover, the outlier threshold was set to 5°, whereby any data samples with high angular errors above the pre-set threshold will be discarded. This could reduce the effect of human error, such as closing the eyelid or moving eyes away from calibration markers, in influencing the measurement. To evaluate the data quality, a few mathematical functions were involved to assess the quality of recorded data in terms of angular accuracy, angular precision, and data loss similar to the approach described in the study by Niehorster, et al. (2020) and Chan (2021). Every measurement was calculated separately for each task in each participant's recording. The computed mathematical values indicate whether the developed eye tracker can be reliably employed for the colour detection application to accurately and precisely locate the gaze. Table 3.4 illustrates the description of each mathematical function being employed in evaluating the performance of the eye tracker.

Table 3.4: Mathematical Functions Employed in Performance Evaluation.

Mathematical Computations	Description
Deviation	To quantitatively evaluate the accuracy, deviation is used to compute the average angular distance (in degrees of visual angle) between fixation locations and corresponding locations of the fixation targets.
Root-Mean-Square of Sample-to-Sample (RMS-S2S)	To quantitatively assess the precision, RMS-S2S is employed to calculate the angular distance (in degrees of visual angle) between succeeding fixation samples.
Data Loss	Number of missing samples is calculated based on confidence value and expressed as a percentage of the number of expected samples in a recoding interval which can be obtained from Pupil Capture log history.

3.6.2   Colour Detection Plugin

3.6.2.1   Colour Detection using RGB Values (Version 1)

Five colours will be chosen from the RGB colour chart, which includes Lavender Blue (#CCCCFF), Snowy Mint (#CCFFCC), Electric Yellow (#FFFF33), Pale Red (#FFCCCC), and Mauve (#CC99FF). The colours will be displayed using an external monitor screen to allow ongoing monitoring of the RGB value recorded by the camera. Participants will be instructed to maintain their gaze at the centre of the colour displayed while the RGB values are recorded accordingly. To assess the performance of the detection, the percentage error will be calculated for each RGB value, and the mean percentage error will be computed subsequently. The overall performance will then be presented in terms of the percentage error by calculating the average percentage error for the five tested colours.

3.6.2.2   Colour Detection using HSL Values (Version 2)

All colours in the pre-classified colour categories, classified by their respective hue, saturation, and lightness values, will be utilized to assess the performance of the developed colour detection plugin. Furthermore, the evaluation process will include an additional set of four colours (dark red, brown, dark green, and dark blue) which are not included in the pre-categorized colour categories. To ensure precise configuration with the reference colours, all selected colours will be printed using a laser printer.

To test for the accuracy of colour detection, the assessment will be repeated three times for each participant under different lighting settings (bright, natural, and dark) while the colour will be displayed 20 cm in front of the participant. Different lighting conditions could also provide information on how the light variation contributes to the deviation of the detection's accuracy. The same light source will be employed in the testing to ensure the reliability of the results. When the participant is right beside the light source, it is defined as a bright condition, followed by a natural condition when the participant is 3 meters away from the light source, and a dark condition when the participant is 6 meters away from the light source.

The performance of the colour detection plugin was evaluated in terms of accuracy. The accuracy was defined as the ratio of the number of correct

colour detections to the total number of observations. The mean accuracy was also calculated using Equation 3.1 to obtain the average performance of the colour detection in three different lighting conditions. Equation 3.3 was employed in computing the accuracy for each colour.

$$Accuracy = \frac{Number\ of\ Correct\ Colour\ Detections}{Total\ Number\ of\ Observations} \times 100\% \quad (3.3)$$

3.7   Summary

To summarise, hardware and software were equally important in the development of wearable eye trackers. Hardware setup will be done before proceeding to gaze detection. Examples of hardware setup include the modification of the camera module, fabrication of the mounting platform, construction of IR LEDs onto the camera module, and the removal of the IR filter from the lens of the camera module. Besides, there will be several significant steps in gaze detection. Hardware settings, such as laptop setup and mounting headset adjustments, will first be executed, followed by the software settings, which include the fine-tuning for pupil detection, calibration, data processing and data analysis on calibrated data. Data collection will be performed for gaze detection once both the required processes in hardware and software settings are done. Moreover, a colour detection plugin will be developed to provide real-time colour detection in the application of an eye tracker. HSL colour space was being utilized in developing the plugin as is less affected by the light variations compared to RGB colour space. The performance of the eye tracker will be evaluated by executing a series of tasks that mimic non-movement settings, facial movement and expression conditions, and head movements in different directions.

CHAPTER 4

RESULTS AND DISCUSSION

4.1 Introduction

This chapter will discuss the evaluation of the developed wearable eye tracker. Section 4.2 will illustrate the final designs of the detachable components in constructing the eye tracker. Several additional considerations employed in developing the eye tracker will also be discussed in this section. Next, Section 4.3 discusses the performance of the developed eye tracker in terms of angular accuracy, angular precision, and data loss, while Section 4.4 compares the results with the study by Chan (2021). Section 4.5 will compare the cost and weight of the developed prototype with various eye trackers in the market. Section 4.6 will illustrate the performance of the developed colour detection plugin. Lastly, Section 4.7 will discuss about the application of colour detection in wearable eye tracker.

4.2 Finalised Designs for a Wearable Eye Tracker

4.2.1 Design Enhancements of Detachable Components for Wearable Eye Tracker

All the designs have been finalised after several changes and improvements. Precise and accurate dimensions are essential in customising the components for the construction of the prototype. Firstly, the dimensions of the hole for both the eye and world camera mounting were measured precisely to ensure that the camera modules could fit completely onto the mounding while screws and nuts could better secure the modules in place. In addition, a smaller opening was designed for eye camera mounting to maximise the infrared light from the IR LED reaching the user's eye for optimal reflection at the eye. Figures 4.1 and 4.2 show the designs of the eye camera mounting and world camera mounting, respectively.
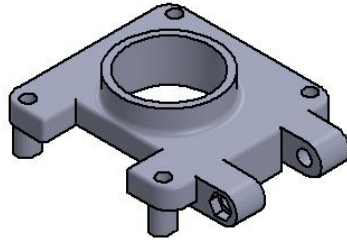
Figure 4.1: Eye Camera Mounting.
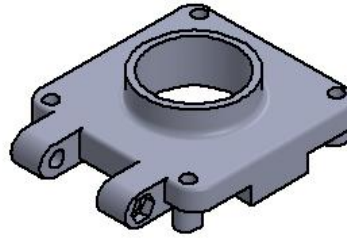
Figure 4.2: World Camera Mounting.

Furthermore, the hinge arm design was improvised by adding certain angular adjustments. This modification facilitated a slight lowering of the eye camera placement relative to the conventional line of sight. This adjustment effectively positioned the user's eye at the focal centre of the eye camera view in Pupil Capture software and minimised the obstruction to the user's sight due to the eye camera. Figures 4.3 and 4.4 illustrated the hinge arm with 10° and 15° angular adjustments, respectively.
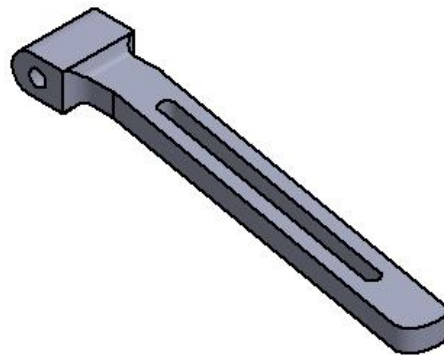
Figure 4.3: Hinge Arm (10°).
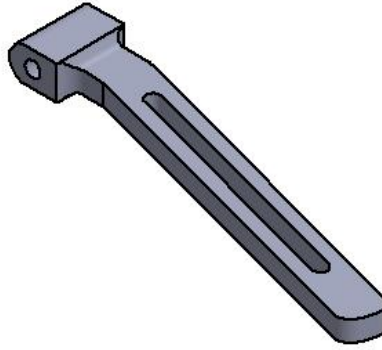
Figure 4.4: Hinge Arm (15°).

Other than that, the extender arm also underwent design changes. The enclosed design was altered to an open design when inserting the hinge arm. This enclosed design was eliminated as the nozzle size of the 3D printer was limited, which failed to properly construct the design. Additionally, the open design allowed the user to attach the hinge arm to the extender arm more easily by using screws to secure them together. Two rectangular holes were designed to allow the securing of the extender arm onto the frame using magic tape. Figures 4.5 and 4.6 show the design of the extender arm with different angular settings.

Figure 4.5: Extender Arm (10°).

Figure 4.6: Extender Arm (20°).

The world camera hinge was designed to establish a secure connection between the frame and the world camera mounting. A useful design feature was included in the camera hinge in order to reduce any potential closeness issues between the camera module and the user's forehead. By slightly extending the camera hinge forward, this design feature reduced the discomfort brought on by contact between the camera module and the user's forehead. Additionally, this forward extension enabled better air circulati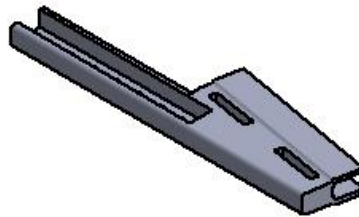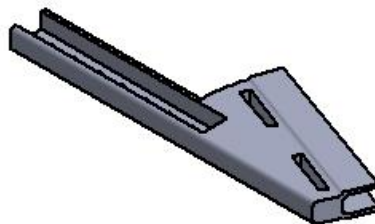on, which efficiently dissipates heat and ensures the camera module cools down to the ideal temperature, especially after longer periods of use. Similarly, two small rectangular holes were designed to allow the tightening of the world camera hinge onto the frame using magic tape. Figure 4.7 shows the design of the world camera hinge.
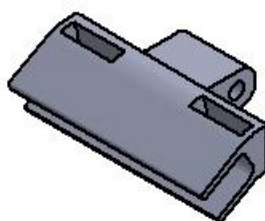
Figure 4.7: World Camera Hinge.

4.2.2   Additional Fabrication Actions Involved

As the raw material for 3D printing was limited in the laboratory, a spectacle-like frame from a face shield was chosen for its flexible and lightweight qualities. Additionally, the cost of this frame was significantly lower than a 3D-printed one. Besides, A small, portable polishing machine was used as part of the fabrication process to provide the 3D-printed components with the required level of fineness and accuracy. This process made sure that all finished structures met all the necessary standards and specifications. Specific modifications were also carried out to the original frame design to allow proper integration of the eye tracker components. Particularly, the frame's right temple underwent careful polishing to enable a secure fit with the extender arm, improving the wearable device's overall functionality and physical appearance.

Moreover, rubber eyeglass stoppers were positioned on both temples of the frame to enhance user comfort and the stability of the eye tracker throughout its application. These stoppers offered a firm hold on the user's ears,

which then effectively reduced the possibility of unwanted movement as well as slippage issues. A do-it-yourself approach was used to create a comfortable and functional nose pad through the creative application of EVA foam and super glue. This method not only prioritises user comfort but also ensures the reliability of the prototype.

A practical decision has been made to employ nylon magic tape for securing two components, the extender arm and world camera hinge, to the frame. This setup ensured a secure and flexible attachment, contributing to the wearable eye tracker's overall performance and reliability. Wire holder clips have been modified to attach to the frame in order to deal with the wire management issue and provide user convenience. This innovative modification minimised the discomfort brought on by the cables' presence while also lowering the possibility of unintentional wire pulling. Additionally, it improved the device's visual appeal by giving it a neat and organised appearance.

4.2.3   Final Prototype

Figure 4.8 shows the final prototype, whereby the eye and world camera modules are attached to the customized mounting and secured to the frame using the designed hinge arm, extender arm, and world camera hinge.
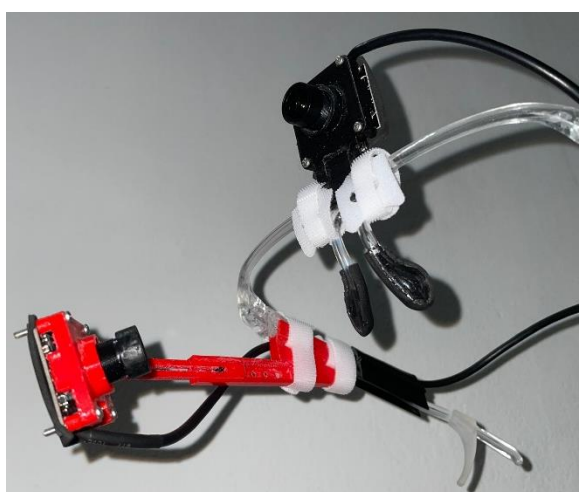
Figure 4.8: Final Prototype for Wearable Eye Tracker.

4.3   Performance of Eye Tracker

Data was collected from a cohort of five participants, each performing seven designated tasks with three repetitions per task. This resulted in a total dataset

comprising 105 observations related to angular accuracy, angular precision, and data loss. Subsequently, means and standard deviations were calculated based on this gathered dataset.

4.3.1 Calibration Results between Unfreeze Model and Freeze Model

Figure 4.9 showed the evaluation of calibration results between unfreeze model and freeze model in terms of angular accuracy, angular precision, as well as data loss.
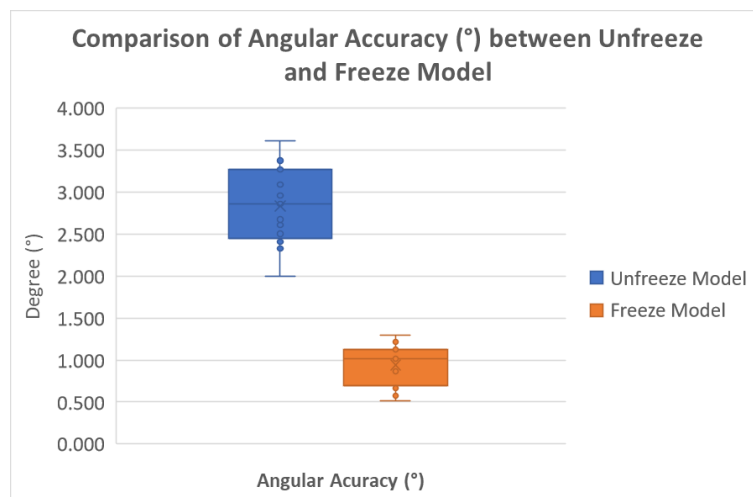
(a)
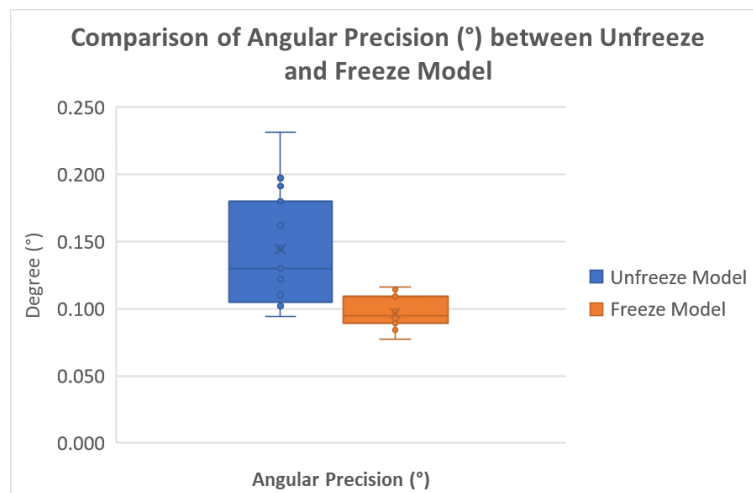
(b)
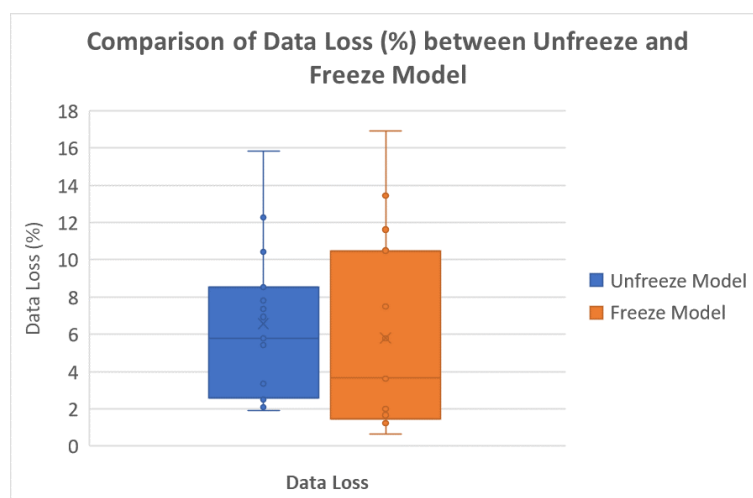
(c)

Figure 4.9: Comparison of Calibration Results between Unfreeze Model and Freeze Model in terms of Angular Accuracy (a), Angular Precision (b), and Data Loss (c).

The results showed that the unfreeze model exhibited a significantly greater noise level with angular accuracy of $2.833° \pm 0.441°$, whereas the freeze model showed a reduced noise level and improved angular accuracy of $0.939° \pm 0.229°$. The freeze model also demonstrated better angular precision, with an error rate of $0.9°$, than the unfreeze model, which had a greater error rate of $1.5°$. Yet, it is important to note that the freeze model experienced a greater deviation in the data loss compared to unfreeze model.

According to the observations, freezing the model could result in significant improvements in gaze estimation stability, which would extensively lower both noise and errors. Yet this advantage is offset by some data loss. In contrast, the unfreeze model has a lower rate of data loss while demonstrating slightly decreased accuracy and precision. It demonstrates a capacity to adapt, allowing it to take into account changes like slippage over time. GitHub (n.d.) stated that there is a trade-off between stability (the freeze model) and adaptability (the unfreeze model). These models must be selected depending on the specific use case and environmental context. To elaborate, a freeze model is employed for controlled laboratory studies, where head movement is restricted, to provide better accuracy and precision when the data loss is less critical. Meanwhile, the unfreeze model is selected for application in natural situations,

where head or eye movement is involved, to adapt better even with slightly lower accuracy and precision, as lower data loss is crucial.

4.3.2 Comparison of Angular Accuracy (°), Angular Precision (°), and Data Loss (%) with Respective Tasks using Freeze Model

Figure 4.10 shows the overview of the performance evaluation for all seven tasks in terms of angular accuracy, angular precision, and data loss. The details will be discussed in the following parts.
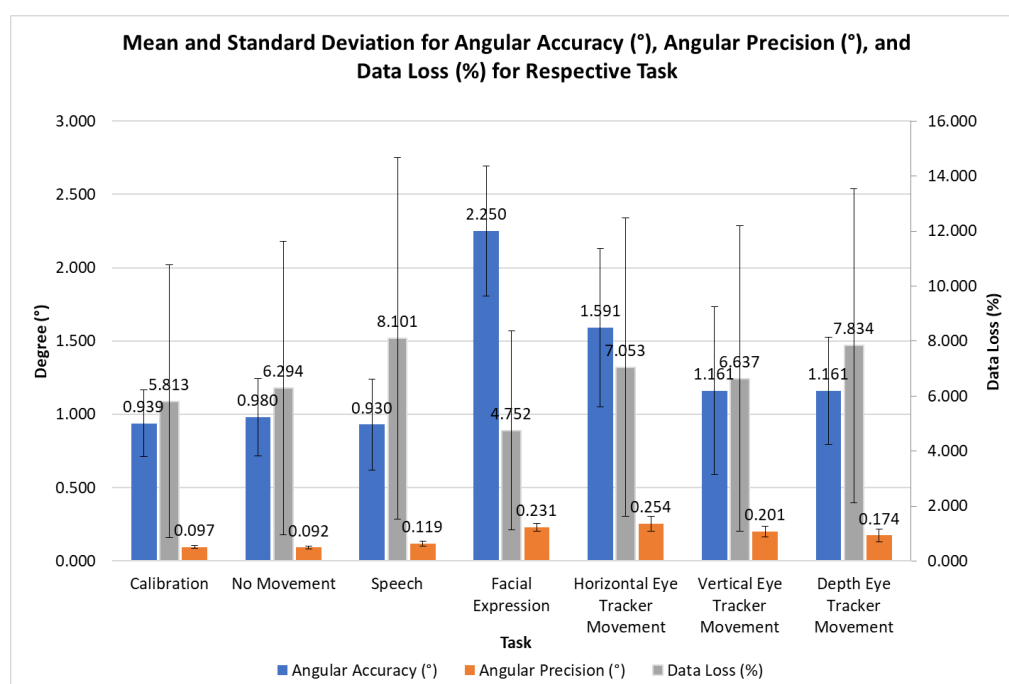
Figure 4.10: Overview of Performance Evaluation for All Tasks.

4.3.2.1 Non-Movement Tasks

Figure 4.11 illustrates the results of assessment for non-movement tasks.
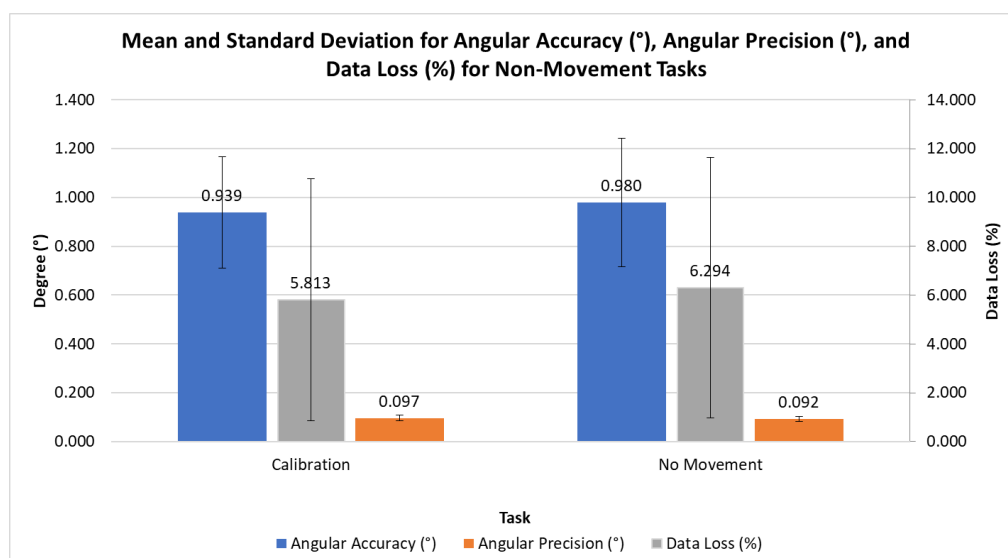
Figure 4.11: Results for Non-Movement Tasks.

It is evident that there was no significant difference in the angular accuracy, angular precision, or data loss for Tasks (1) and (2). In particular, the angular accuracy showed a low variation, measuring at 0.939° for calibration and 0.980° for no movement. Similarly, the angular precision displayed close values, registering at 0.0.97° in the calibration task and 0.092° in the no movement task. There was little increase in the data loss, measuring at 5.813% and 6.294% for calibration and no movement tasks, respectively. Given that both tasks included stable settings that are naturally favourable to the freeze model's best performance, this stability in accuracy, precision, and data loss is consistent with the explanation in the comparison between the unfreeze and freeze models.

The little increase observed in both angular accuracy and data loss, along with their standard deviations, may be attributed to the run-to-run variability in evaluations of this nature. Additionally, it is worth considering that the increase in sample duration for the non-movement task, which doubled compared to the regular calibration task, might have contributed to the noticed changes in accuracy and data loss. This extension could have potentially resulted in decreased attentiveness or increased fatigue among participants, leading to a reduced confidence level during testing and eventually establishing variations in accuracy and data loss. According to Lin, et al., (2022), total fixation time duration was found to be the most sensitive parameter for visual

fatigue within the accuracy score. The average longest continuous duration of inner circle viewing time decreased from 5.3 sec to 2.5 sec after the fatigue task, and the average accuracy score fell to 35.6 scores from 54.8 scores (Lin, et al., 2022). These findings emphasise that visual fatigue can be due to fixation duration, which then results in changes in accuracy and data loss.

4.3.2.2 Facial Movement and Expression Tasks

Figure 4.12 shows the results of evaluation for facial movement and expression tasks.
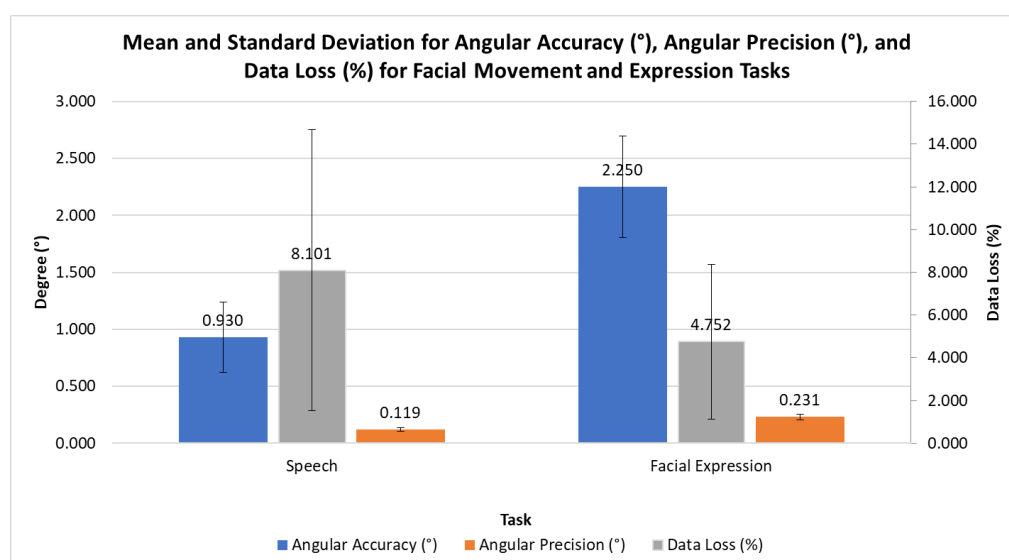
Figure 4.12: Results for Facial Movement and Expression Tasks.

The results clearly indicate that the standard deviations associated with angular accuracy, angular precision, and data loss considerably increase when comparing the facial movement and expression tasks to non-movement tasks. It is logical to assume that the little facial movements that involve the muscles of the face were what caused the observed increase in variability. These little face movements during testing produce motion artefacts, which eventually lead to the variations in measurements that are seen.

A comparison of the results from tasks involving speech and facial expressions reveals that facial expressions, particularly the action of lifting the eyebrows, tend to produce more noticeable movement artefacts than the speech task. The result of such events was a greater degree of deviation in angular

accuracy and data loss. Contrarily, it is noticeable that facial emotions produce better outcomes when angular precision is examined. This improvement is likely due to the fact that lifting the eyebrows largely involves a vertical eye tracker movement as opposed to the multidirectional movement required for speaking activities.

Furthermore, a more extreme level of angular accuracy deviation was seen in the facial expression task, specifically the act of lifting the eyebrows. This difference can possibly be attributed to the mounting platform's construction, in which the nose support is carefully positioned around the base of the nose. This particular positioning causes noticeable skin movement when the eyebrows are elevated, in contrast to placing the nose support at the nasal bridge.

4.3.2.3 Head and Eye Tracker Movement Tasks

Figure 4.13 demonstrates the results of the assessment for head and eye tracker movement tasks.
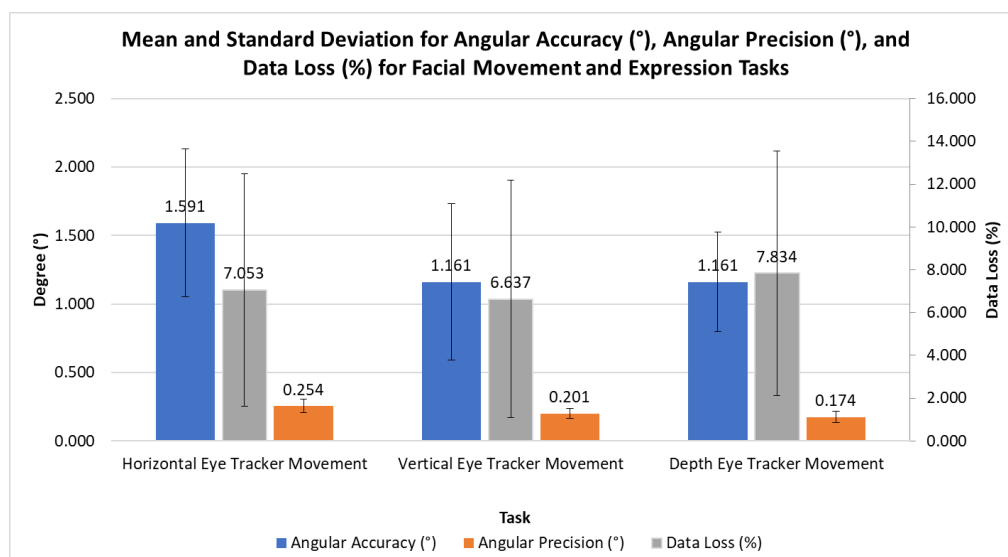
Figure 4.13: Results for Head and Eye Tracker Movement Tasks.

When comparing tasks involving head and eye tracker movement to those requiring no movement, the results clearly showed a substantial rise in the degree of deviation regarding angular accuracy and precision, as well as data loss. It is also interesting that tasks involving head and eye tracker movement

show a considerable rise in the standard deviations related to these parameters. The findings might be explained by the generation of head movement artefacts, which could then induce slight slippage effects during the collection of data.

Additionally, the world camera's relatively lower resolution and frame rate should be taken into account because they may introduce errors into the processing pipeline used for data processing. The world camera module's very small field of vision, which covers around 90 degrees, could also be an important issue. This narrow field of vision may cause errors and data loss since the world camera may stray from calibration markers inside it, especially during head and eye tracker movement activities.

4.4 Comparison in Calibration Results between Chan (2021) and This Study

Figure 4.14 and Table 4.1 illustrate the comparison in calibration results between the study by Chan (2021) and this study.
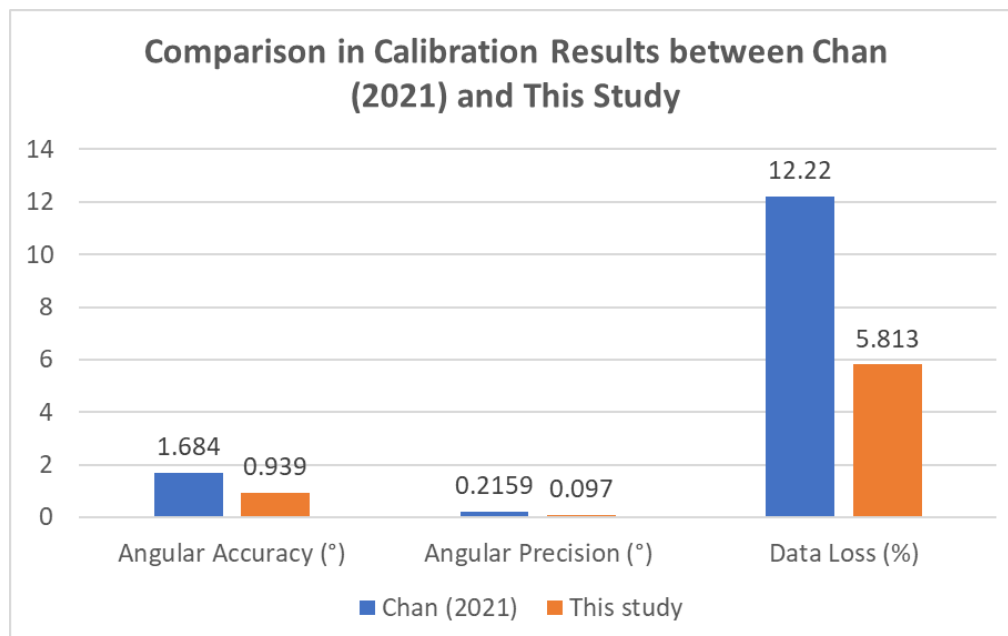
Figure 4.14: Comparison in Calibration Results between Chan (2031) and This Study.

Table 4.1:   Comparison in Calibration Results between Chan (2021) and This
Study.

	Mean		Percentage Difference (%)
	Chan (2021)	**This study**	
Angular Accuracy (°)	1.684	0.939	44.21
Angular Precision (°)	0.2159	0.097	55.29
Data Loss (%)	12.22	5.813	52.43

Significant improvements in the performance of the eye tracker were observed compared to Chan (2021) in terms of angular accuracy and precision as well as data loss. The angular accuracy and precision were improved by about 50%, while the data loss was minimised by 52.43%.

One of the possible factors that contribute to such improvements is the employment of the freeze model. This model provides better stability in accuracy and precision when the tasks do not involve significant movements. Besides, designs that minimise the potential eye tracker movement and slippage issue could lead to great improvements. Several design considerations were taken into account to improve the prototype, particularly the nose pad and rubber eyeglass stopper, which could be factors that enhance the overall performance of the developed wearable eye tracker.

4.5   Cost and Weight Comparison with Various Eye Trackers

The final prototype equipped with a frame, camera modules, an IR LED, 3D printed components, screws, and nuts showed a significant decrease in the built-up cost compared to the prototype done by Chan (2021). Additionally, the prototype in this study was also slightly lighter than the one by Chan (2021). Table 4.2 shows the cost and weight differences between the prototype in this study and the one from Chan (2021). In addition, Table 4.3 compares the low-cost prototype developed in this study with various eye trackers on the market.

Table 4.2: Cost and Weight Comparison with Chan (2021).

	Chan (2021)	This Study	Changes (+/-)
Cost (RM)	132.00	76.84	-55.16
Weight (g)	69.5	65.6	-3.9

Table 4.3: Cost and Weight Comparison with Various Eye Trackers.

	Cost (RM)	Weight (g)
Pupil Labs Headset	12150	22.75 (Only Frame)
Tobii Pro Glasses 2	41645	45
This Study	76.84	65.6

Significant cost savings in the prototype construction were achieved through a thoughtful decision in camera module selection. The trade-off for selecting cost-effective camera modules was a compromise in camera resolution. Both camera modules employed in the prototype delivered images at a resolution of 1280×720 pixels, remarkably lower than the specifications reported by Chan (2021), which featured 5 Megapixels for the world camera and 2 Megapixels for the eye camera. Nevertheless, the resolutions offered by the low-cost camera modules remained acceptable for the intended purpose, as they successfully captured the fundamental shapes of objects without requiring fine-detail precision.

4.6   Performance Evaluation of Developed Colour Detection Plugin

4.6.1   Colour Detection using RGB Values (Version 1)

Five colours were selected for assessing the performance of colour detection that utilised the captured RGB values. Percentage error was employed to calculate the difference between the actual and recorded RGB values. Table 4.4 shows the percentage error for colour detection using RGB values.

Table 4.4:   Percentage Error for Colour Detection using RGB Values

Colour		RGB Value		Percentage Error	Mean Percentage Error
		Actual	Recorded		
Lavender Blue	R	204	128	37.25	
	G	204	193	5.39	14.22
	B	255	255	0.00	
Snowy Mint	R	204	155	24.02	
	G	255	226	11.37	18.33
	B	204	244	19.61	
Electric Yellow	R	255	186	27.06	
	G	255	200	21.57	22.09
	B	51	42	17.65	
Pale Red	R	255	187	26.67	
	G	204	203	0.49	16.90
	B	204	252	23.53	
Mauve	R	204	128	37.25	
	G	153	193	26.14	21.13
	B	255	255	0.00	
			Overall Percentage Error		18.53

As there were millions of RGB combinations, a little movement in the gaze could cause significant changes in the RGB values. Hence, this algorithm was not able to capture the RGB values accurately. In addition, the evaluation of the colour detection was not convincing as it was done by computing the percentage error between actual and recorded RGB values, and the performance was determined by the overall percentage error. None of the studies have utilised the same assessment approach (Version 1) for colour detection. Therefore, this approach was improvised to involve HSL in detecting the colours.

4.6.2   Colour Detection using HSL Values (Version 2)

A total of five participants were recruited to take part in the evaluation of the newly developed colour detection plugin. Each participant underwent three

separate sessions, each conducted under different lighting conditions. Participants were instructed to assess a palette of eighteen different colours. Consequently, this evaluation procedure generated five datasets for each of the chosen colours in each lighting condition, resulting in the use of a set of data including 270 observations for the evaluation of the performance of the colour detection plugin. As the additional four colour sets were not pre-classified in the colour detection plugin, they were excluded from the computation of accuracy. However, the colours detected from these additional colour sets were recorded to assess the reliability of the developed colour detection plugin. Table 4.5 shows the accuracy in correctly identifying the chosen colour under different lighting settings and the average accuracy of the colour detection under each lighting condition.

Table 4.5:   Accuracy of Colour Detection under Various Lighting Conditions.

Colour	Accuracy (%)			
	Bright	Natural	Dark	Average
Red	100	100	100	100.0
Pink	100	100	100	100.0
Orange	100	100	100	100.0
Gold	60	100	40	66.7
Yellow	100	100	100	100.0
Yellow-Green	100	100	100	100.0
Green	100	60	20	60.0
Spring Green	100	100	20	73.3
Blue	100	100	40	80.0
Cyan	100	100	40	80.0
Purple	60	60	20	46.7
Black	100	100	100	100.0
Gray	100	100	100	100.0
White	60	40	0	33.3
Mean Accuracy for Each Lighting Condition	91.4	90.0	62.9	

Several important insights were produced from the analysis of the colour detection accuracy. Firstly, the colour detection exhibited excellent performance under bright and natural lighting conditions, achieving average accuracies of 91.4% and 90%, respectively. Nevertheless, its performance declined significantly in darker settings, with an accuracy rate of 62.9%.

Certain colours, such as red, pink, orange, yellow, yellow-green, black, and grey, consistently achieved 100% accuracy across all lighting conditions, which underlines the correctness of these specific hues. In contrast, colours like green, spring green, blue, and cyan demonstrated high accuracy in well-lit environments but suffered decreased performance in dimmer conditions. This suggests a potential sensitivity to lighting variations for these colours.

Moreover, colours like gold, purple, and white exhibited lower overall accuracy. They were identified as other hues close to them under certain lighting conditions. This can be due to the low-cost camera sensor's inability to accurately capture the RGB values produced from the displayed colours. Purple showed an average accuracy of about 45% across situations and so appeared to be a difficult colour for the model to determine. Additionally, white detection accuracy has obviously decreased, particularly in natural and dim settings. This may be due to the developed algorithm for determining white, which highly depends on lightness.

The findings clearly demonstrate the significant impact of lighting conditions on colour detection accuracy, with the best results being shown in strong natural light. In areas with poor lighting, the potential inclusion of additional lighting could improve accuracy. Furthermore, the high accuracy on saturated primary colours does not extend well to light or dark shades. Hence, this explains that the detection depends on colour brightness. This could be due to the designed detection algorithm, where saturation and lightness will be first considered when identifying colours rather than considering all the hue, saturation, and lightness together. As a whole, the plugin continues to function quite well under ideal conditions, although it has significant limits in less bright environments.

Other than the pre-classified colours, four additional colours were chosen to assess the performance of the colour detection. Since these colours were not pre-identified in the development of the plugin, it was expected that

there would be no exact match for the colours identified. Table 4.3 recorded the colour detected for respective colours in different lighting conditions.

Table 4.6:   Results of Colour Detection for Additional Colour Sets under Various Lighting Conditions.

Colour	Colour Identified		
	Bright	**Natural**	**Dark**
Dark Red	Red	Red	Black
Brown	Yellow	Orange	Black
Dark Green	Green	Black	Black
Dark Blue	Blue	Black	Black

Dark colour variations, such as dark red, brown, dark green, and dark blue, pose more difficulties for reliable identification, especially in low light. Dark green and dark blue were classified as black in natural lighting conditions, but dark red retained its identity as red even under natural lighting conditions. Brown was identified as either yellow (in bright lighting) or orange (in natural lighting). This can be explained by the fact that brown is a composite colour made up of red, yellow, and orange hues (Cabral, 2019). Although dark green is identified well in bright light settings, it is frequently registered as black in both natural and low-light situations. Similarly, dark blue is correctly identified in bright conditions but tends to be misidentified for black in darker settings. These observations indicate that the camera employed does not have a good auto-light correction module.

In a general context, it becomes obvious that these darker colour variations tend to trigger higher occurrences of misidentification, particularly in low-light settings. This emphasises the algorithm's dependence on factors like brightness and saturation.

4.7   Application of Colour Detection in Eye Tracker

The significant improvements in terms of angular accuracy and precision, as well as data loss, demonstrate that the developed wearable eye tracker is reliable in providing gaze estimation. Similarly, the results show that the colour

detection functions as intended in bright and natural lighting conditions, but performance worsens in dark environments. Hence, it is still mostly reliable, provided the application happens in environments with sufficient lighting. In order to be completely reliable, a more detailed hue range might be required to properly classify the colours accordingly.

In general, a colour detection plugin developed in the eye tracker could be a game charger for individuals with colour blindness. Firstly, this plugin could help identify colours accurately as it shows great accuracy in bright and natural lighting settings. This would be particularly useful in situations where accurate colour recognition is necessary, such as reading maps, graphs, or other visual data. In addition, real-time colour detection could allow users who suffer from colour blindness to be aware of the signs and warning labels that can be simply found in the surroundings. To elaborate, the Occupational Safety and Health Administration (OSHA) has recommended that the signs or tags for danger be red, caution be yellow, warning be orange, biological hazard be orange-red, safety instructions be green, and slow-moving vehicles be fluorescent yellow-orange (The Ohio State University, 2020).

Besides, eye trackers equipped with real-time colour detection can help researchers understand how humans see in colour. This can lead to new treatments for colour blindness and potentially allow researchers to enhance human colour perception (Mukamal, 2017). Additionally, it could possibly allow the parents or carers to identify the possibility of colour blindness in the children at an early stage, which then allows for early diagnosis or relevant treatment if necessary. Other than that, it could also aid in educational settings, allowing students with colour blindness to fully engage with visual learning materials (International Specialist Eye Centre Malaysia, n.d.). Burton (2021) stated that colours are crucial in stimulating learning progress because 60% of the human brain is granted to process visual information, which could potentially increase the learning speed of an individual. The real-time colour detection that provides feedback on the colour of the fixated object can then enhance the learning process for individuals with colour blindness.

4.8 Summary

In summary, the implementation of the frozen model yielded a substantial enhancement in gaze estimation stability. However, this came at the cost of some data loss. In tasks where no movement occurred, there emerged slight differences in accuracy, precision, and data loss between calibration and no movement tasks. Facial movements, such as those associated with speech and expressions, establish increased measurement variability owing to motion artefacts. Particularly, the raising of eyebrows induced more pronounced deviations compared to speech-related movements. Additionally, head and eye tracker movements resulted in significant deviations in accuracy, precision, and data loss, primarily due to motion artefacts and slippage effects. In a comparative context with the study by Chan (2021), this prototype exhibited remarkable improvements, with over a 50% enhancement in angular accuracy and precision and a corresponding 52% reduction in data loss. These advancements can be attributed, in part, to design refinements like the nose pad. Besides, this prototype was achieved at a considerably lower cost than commercial choices, necessitating trade-offs in camera selection. It also exhibited a slightly reduced weight in comparison to the previous prototype in Chan (2021).

Regarding the colour detection plugin, it exhibited accuracy rates exceeding 90% under bright and natural lighting conditions, but this dropped to 63% accuracy in dim settings. While primary saturated colours were reliably detected, the differentiation of lighter and darker shades presented greater challenges. The application of colour detection could help individuals who suffer from colour blindness identify colours correctly, potentially allowing researchers to enhance human colour perception and result in new treatments as well as enhance the learning process.

CHAPTER 5

CONCLUSIONS AND RECOMMENDATIONS

5.1   Conclusions

In conclusion, this study has successfully designed and developed an affordable, wearable eye tracker prototype. The prototype utilised low-cost hardware components like web camera modules and 3D-printed mounting structures. The built-up cost of this prototype was RM 66.34, whereby the substantial cost savings in the prototype construction were achieved through a thoughtful decision in camera module selection. To ensure the reliability of the prototype, mounting headset adjustments and fine-tuning for pupil detection as well as calibration are essential before actual application to achieve the ideal performance. The prototype exhibited excellent angular accuracy (0.939°) and precision (0.097°) in controlled non-movement conditions. However, facial movements and expressions generated motion artefacts that increased variability in measurements. Similarly, head and eye tracker movements produced substantial deviations in accuracy, precision, and data loss due to motion artefacts and slippage effects. Besides, performance evaluation demonstrated major improvements compared to the prototype done by Chan (2021), with angular accuracy and precision enhanced by over 50% and data loss reduced by 52%.

Moreover, the colour detection plugin, which utilises HSL colour space, has been developed to provide ongoing feedback on the detected colours according to the gaze location. It achieved high accuracy, exceeding 90% in bright and natural lighting. Further studies and improvements can be made to enhance the performance of colour detection in low lighting environment. Lastly, this prototype demonstrated its reliability by offering a low-cost alternative eye tracker with capabilities for assisting individuals with colour blindness through real-time colour detection. It is believed that such innovation could enhance the learning process for individuals who suffer from colour blindness and enable researchers to improve human colour perception as well as identify better treatments.

5.2   Recommendations for Future Work

To further advance the development of an affordable wearable eye tracker, it is essential to focus on hardware improvements. As the developed eye tracker is connected to a laptop for its application in this study, the size of the personal computer can be further reduced in the future by employing a single-board personal computer, such as a Raspberry Pi or Intel NUC. Furthermore, predictive filtering techniques can be implemented to minimise the impact of motion artefacts induced by user movements.

Besides, improving the camera sensor quality could enable more accurate colour detection, specifically for distinguishing between light and dark shades. In addition, refining the colour detection algorithm by considering factors like hue, saturation, and lightness together rather than relying solely on saturation and lightness could significantly enhance detection accuracy. Also, more studies can be conducted to classify the hue range into more detailed categories.

To address the performance issues in low-light settings, incorporating additional lighting that can be switched on and off by the user, such as surface-mount LEDs, can potentially enhance colour detection. Additionally, audio output functions can be integrated by involving a tiny speaker in the development of the eye tracker to provide auditory information to the user.

Other than that, the user experience should be taken into consideration. This can be achieved by assessing the user experience quantitatively through feedback surveys and qualitatively through interviews. By collecting user feedback, areas for improvement in overall usability can be clearly identified.

Lastly, detailed validation and testing are important parts of future work. The evaluation of the eye tracker's performance can be done on a larger and more diverse participant group, which will help ensure its effectiveness across different user demographics and use cases. Similarly, conducting thorough validation and testing in various real-world scenarios could potentially help refine the device and make it more reliable and accurate.

REFERENCES

Adams, J., Parulski, K. and Spaulding, K., 1998. Color processing in digital cameras. IEEE Micro, [e-journal] 18(6), pp.20 – 30. https://doi.org/10.1109/40.743681

Al-Doweesh, S.A., Al-Hamed, F.A. and Al-Khalifa, H.S., 2014. What Color? A Real-time Color Identification Mobile Application for Visually Impaired People. *Springer eBooks*, pp.203–208. https://doi.org/10.1007/978-3-319-07854-0_36

Altvater-Mackensen, N., 2021. *What Are You Looking At? Using Eye Tracking Glasses to Monitor Toddler Attention in Natural Learning Situations*. In: Danielle Dionne and Lee-Ann Vidal Covas, Proceedings of the 45th annual Boston University Conference on Language Development. Somerville, MA: Cascadilla Press.

Alvino, L., Pavone, L., Abhishta, A. and Robben, H., 2020. Picking Your Brains: Where and How Neuroscience Tools Can Enhance Marketing Research. *Frontiers in Neuroscience*, [e-journal] 14. https://doi.org/10.3389/fnins.2020.577666

Benjamins, J.S., Hessels, R.S. and Hooge. I.T.C., 2018. GazeCode: open-source software for manual mapping of mobile eye-tracking data. ETRA, pp. 1 – 4.

Best, V., Boyd, A.D. and Sen, K., 2023. An Effect of Gaze Direction in Cocktail Party Listening. *Trends in Hearing*, [e-journal] 27. https://doi.org/10.1177/23312165231152356

Biondi, M., 2021. *4 key benefits of eye tracking to highlight in your grant proposal*, [online] 21 March. Available at: <https://www.tobii.com/blog/4-key-benefits-of-eye-tracking> [Accessed 3 March 2023].

Bojko, A., 2013. *Eye Tracking the User Experience: A Practical Guide to Research*. Rosenfeld Media, Brooklyn, New York.

Bradley, S., 2013. The Fundamentals of Color: Hue, Saturation, And Lightness. [online] Available at: <https://vanseodesign.com/web-design/hue-saturation-and-lightness/> [Accessed 10 June 2023].

Brunye, T.T., Drew, T., Weaver. D.L. and Elmore, J.G., 2019. A review of eye tracking for understanding and improving diagnostic interpretation. *Cognitive Research: Principles and Implication*, [e-journal] 4. https://doi.org/10.1186/s41235-019-0159-2

Burton, 2021. *How Do Colors Influence Learning?* Thinkific, [blog] 28 January. Available at: <https://www.thinkific.com/blog/how-colors-influence-learning/#:~:text=While%20there%20are%20several%20factors,the%20brain%2C%E2%80%9D%20she%20says> [Accessed 16 September 2023].

Cabral, C., 2019. *What Colors Make Brown? How to Make 5 Common Shades*. PrepScholar, [blog] 3 September. Available at: <https://blog.prepscholar.com/what-colors-make-brown> [Accessed 16 September 2023].

Chan, H., 2021. *Development of a Wearable Eye Tracker to Control an Autonomous Wheelchair*. Degree. Universiti Tunku Abdul Rahman.

Chugh, S., Brousseau, B., Rose, J. and Eizenman, M., 2021. *Detection and Correspondence Matching of Corneal Reflections for Eye Tracking Using Deep Learning*. 2020 25th International Conference on Pattern Recognition (ICPR). Milan, Italy, 10-15 January 2021. IEEE.

Clflores, 2018. *Light and Infrared Radiation*. [online] Available at: <https://ehs.lbl.gov/resource/documents/radiation-protection/non-ionizing-radiation/light-and-infrared-radiation/#:~:text=We%20experience%20IR%20radiation%20every,welding%20arcs%2C%20and%20plasma%20torches> [Accessed 23 March 2023].

Delabarre, E.B., 1898. A method of recording eye-movements. *The American Journal of Psychology*, 9(4), pp. 572-574.

Dierkes, K., Kassner, M. and Bulling, A., 2018. A novel approach to single camera, glint-free 3D eye model fitting including corneal refraction. *Proceedings of the 2018 ACM Symposium on Eye Tracking Research & Applications*, (9), pp. 1 – 9. https://doi.org/10.1145/3204493.3204525

Dierkes, K., Kassner, M. and Bulling, A., 2019. A fast approach to refraction-aware eye-model fitting and gaze prediction. *Proceedings of the 11th ACM Symposium on Eye Tracking Research & Applications*, [e-journal] (23), pp. 1 – 9. https://doi.org/10.1145/3314111.3319819

Du Plessis, J.-P. and Blignaut, P., 2016. Performance of a simple remote video-based eye tracker with GPU acceleration. *Journal of Eye Movement Research*, [e-journal] 9(4). https://doi.org/10.16910/jemr.9.4.6.

Eynde, M.V. and Puyvelde, P.V., 2017. 3D Printing of Poly(lactic acid). In: Di Lorenzo, M., Androsch, R, Industrial Applications of Poly(lactic acid). *Advances in Polymer Science*, 282. https://doi.org/10.1007/12_2017_28

Farnsworth, B., 2022a. *Eye Tracker Prices – An Overview of 15+ products*, [online] 9 August. Available at: <https://imotions.com/blog/learning/product-news/eye-tracker-prices/>[Accessed 3 March 2023].

Farnsworth, B., 2022b. *Eye Tracking: The Complete Pocket Guide*. [online] Available at: <https://imotions.com/blog/learning/best-practice/eye-tracking/> [Accessed 3 March 2023].

GitHub, n.d. *Release Pupil Capture, Player, and Service release · pupil-labs/pupil*. [online] Available at: <https://github.com/pupil-labs/pupil/releases/tag/v3.4> [Accessed 15 September 2023].

Gwizdka, J., Zhang, Y. and Dillon, A., 2019. Using the eye-tracking method to study consumer online health information search behaviour. *Aslib Journal of Information Management*, [e-journal] 71(6), pp.739 – 754. https://doi.org/10.1108/AJIM-02-2019-0050

Hansen, D.W. and Ji, Q., 2010. In the Eye of the Beholder: A Survey of Models for Eyes and Gaze. *IEEE Transactions on Pattern Analysis and Machine Intelligence*, [e-journal] 32(3), pp. 478 – 500. https://doi.org/10.1109/TPAMI.2009.30

Holmqvist, K., Nystrom, M., Andersson, R., Dewhurst, R., Jarodzka, H. and van de Weijer, J., 2011. *Eye Tracking: A Comprehensive Guide to Methods and Measures*. Oxford University Press, Oxford.

Huey, E.B., 1898. Preliminary experiments in the physiology and psychology of reading. *The American Journal of Psychology*, 9(4), pp. 575-586.

iMotions, n.d.a. *Eye Tracking Glasses*. [online] Available at: <https://imotions.com/products/imotions-lab/modules/eye-tracking-glasses/#Resources> [Accessed 20 February 2023].

iMotions, n.d.b. *Powering Human Insight*. [online] Available at: <https://imotions.com/products/imotions-lab/> [Accessed 22 February 2023].

International Specialist Eye Centre Malaysia, n.d. *Colour Blindness*. [online] Available at: <https://www.isec.my/patientinformation/colour-blindness/> [Accessed 16 September 2023].

Klaib, A.F., Alsrehin, N.O., Melhem, W.Y., Bashtawi, H.O. and Magableh, A.A., 2021. Eye tracking algorithms, techniques, tools, and applications with an emphasis on machine learning and Internet of Things technologies. *Expert Systems with Applications*, [e-journal] 166. https://doi.org/10.1016/j.eswa.2020.114037

Ku, C.H., Kim, S.W., Kim, J.Y., Paik, S.W., Yang, H.J., Lee, J.H. and Seo, Y.J., 2020. Measurement of Skull Size on Computed Tomography Images for Developing a Bone Conduction Headset Suitable for the Korean Standard Head Size. *Journal of Audiology and Otology*, [e-journal] 24(1), pp. 17 – 23. https://doi.org/10.7874/jao.2019.00290

Kujur, A., Bhattacharya, A., Sharma, G. and Kumar, J., 2022. *Prediction of Workload under Distraction using Supervised Learning Algorithms*. 2022 3rd International Conference on Issues and Challenges in Intelligent Computing Techniques (ICICT). Ghaziabad, India, 11 – 12 November 2022. IEEE.

Le, T., Tran Hung Son, Mita, S. and Nguyen, T.D., 2010. Real Time Traffic Sign Detection Using Color and Shape-Based Features. Lecture Notes in Computer Science, pp. 267 – 278. https://doi.org/10.1007/978-3-642-12101-2_28

Lee, L., Burnett, A.M., Panos, J.G., Paudel, P., Keys, D., Ansari. H.M. and Yu, M., 2020. 3-D printed spectacles: potential, challenges and the future. *Clinical and Experimental Optometry*, [e-journal] 103(5), pp. 590 – 596. https://doi.org/10.1111/cxo.13042

Li, W., Kearney, P., Braithwaite, G. and Lin, J.J.H., 2018. How much is too much on monitoring tasks? Visual scan patterns of single air traffic controller performing multiple remote tower operations. *International Journal of Industrial Ergonomics*, [e-journal] 67, pp.135 – 144. https://doi.org/10.1016/j.ergon.2018.05.005

Lin, H.-J., Chou, L.-W., Chang, K.-M., Wang, J.-F., Chen, S.-H. and Hendradi, R., 2022. Visual Fatigue Estimation by Eye Tracker with Regression Analysis. *Journal of Sensor*, [e-journal] 2022. https://doi.org/10.1155/2022/7642777

Matthes, R., 2011. *Infrared Radiation*. [online] Available at: <https://www.iloencyclopaedia.org/part-vi-16255/radiation-non-ionizing/item/654-infrared-radiation#:~:text=To%20avoid%20possible%20delayed%20effects,or%20for%20shorter%20periods> [Accessed 22 March 2023].

Mazzanti, V., Malagutti, L. and Mollica, F., 2019. FDM 3D Printing of Polymers Containing Natural Fillers: A Review of their Mechanical Properties. *Polymers*, [e-journal] 11(7). https://doi.org/10.3390/polym11071094

McCurley, A. and Nathan-Roberts, D., 2021. Eye-Tracking Assistive Technology for Hands-Free Computer Navigation. *Human Factors and Ergonomics Society*, [e-journal] 65(1). https://doi.org/10.1177/1071181321651313

Microsoft, n.d. *Get started with eye control in Windows*. [online] Available at: <https://support.microsoft.com/en-gb/windows/get-started-with-eye-control-in-windows-1a170a20-1083-2452-8f42-17a7d4fe89a9#ID0EBD=Windows_11> [Accessed 25 March 2023].

Millan, Y.A., Chaves, M.L., and Barrero, J.C., 2020. *A Review on Biometric Devices to be Applied in ASD Interventions*. 2020 Congreso Internacional de Innovacion y Tendencias en Ingenieria (CONIITI). Bogota, Colombia, 30 September – 02 October 2020. IEEE.

Mukamal, R., 2017. *How Humans See In Color*. [online] Available at: <https://www.aao.org/eye-health/tips-prevention/how-humans-see-in-color> [Accessed 16 September 2023].

Nasir, M.H., Brahin, N.M.A., Aminuddin, M.M.M., Mispan, M.S.M. and Zulkifli, M.F., 2021. Android based application for visually impaired using deep learning approach. *IAES International Journal of Artificial Intelligence (IJ-AI)*, [e-journal] 10(4), pp. 879 – 888. https://doi.org/10.11591/ijai.v10.i4.pp879-888

Netco Extruded Plastics, 2016. *Safety Data Sheet – Polylactide (PLA)*. [online] Available at: https://devel.lulzbot.com/filament/Monofilament%20Direct/SDS/Polylactide%20PLA%20R17009A%20SDS.pdf [Accessed 5 March 2023].

Niehorster, D.C., Santini, T., Hessels, R.S., Hooge, I.T.C., Kasneci, E/ and Nystrom, M., 2020. The impact of slippage on the data quality of head-worn eye trackers. *Behaviour Research Methods*, [e-journal] 52, pp.1140-1160. https://doi.org/10.3758/s13428-019-01307-0

Parandoush, P. and Lin, D., 2017. A review on additive manufacturing of polymer-fiber composites. *Composite Structures*, [e-journal] 182, pp. 36 – 53. https://doi.org/10.1016/j.compstruct.2017.08.088

Pouta, M., Lehtinen, E. and Palonen, T., 2021. Student Teachers' and Experienced Teachers' Professional Vision of Students' Understanding of the Rational Number Concept. *Educational Psychology Review*, [e-journal] 33, pp. 109 – 128. https://doi.org/10.1007/s10648-020-09536-y

Pupil Labs, 2023a. *Open source eye tracking platform*. [online] Available at: https://pupil-labs.com/products/core/ [Accessed 20 February 2023].

Pupil Labs, 2023b. *pye3d Pupil Detection*. [online] Available at: https://docs.pupil-labs.com/developer/core/pye3d/#pye3d-pupil-detection [Accessed 21 February 2023].

Pupil Labs, 2023c. *Pupil Capture*. [online] Available at: https://docs.pupil-labs.com/core/software/pupil-capture/ [Accessed 2 March 2023].

Pupil Labs, 2023d. *Technical Specs & Performance*. [online] Available at: https://pupil-labs.com/products/core/tech-specs/ [Accessed 2 March 2023].

Pupil Labs, 2023e. *Hardware*. [online] Available at: https://docs.pupil-labs.com/core/hardware/ [Accessed 20 March 2023].

Pupil Labs, 2023f. *Best Practices*. [online] Available at: https://docs.pupil-labs.com/core/best-practices/ [Accessed 20 March 2023].

Rantanen, V., Vanhala, T., Tuisku, O., Niemenlehto, P/. Verho, J., Surakka, V., Juhola, M. and Lekkala, J., 2011. A Wearable, Wireless Gaze Tracker with Integrated Selection Command Source for Human-Computer Interaction. *IEEE Transactions on Information Technology in Biomedicine*, [e-journal] 15(5), pp. 795 – 801. https://doi.org/10.1109/TITB.2011.2158321

Rudnicki, T., n.d. *Eye-control Empowers People with Disabilities*. [online] Available at: https://www.abilities.com/community/assistive-eye-control.html [Accessed 3 March 2023].

Schindler, M., Lilienthal, A.J., Chadalavada, R.T. and Orgen, M., 2016. Creativity in the eye of the student. Refining investigations of mathematical creativity using eye-tracking goggles. *Proceedings of the 40th Conference of the International Group for the Psychology of Mathematics Education*, 4, pp.163 – 170.

Shah, J., 2020. *Enabling Smart Scrolling using Eye Tracking Technology*. [online] Available at: https://www.einfochips.com/blog/enabling-smart-scrolling-using-eye-tracking-technology/ [Accessed 15 March 2023].

Socha, V., Vidensky, J., Kusmirek, S., Hanakova, L. and Valenta, V., 2022. *Design of Wearable Eye Tracker with Automatic Cockpit Areas of Interest Recognition*. 2022 New Trends in Civil Aviation (NTCA). Prague, Czech Republic, 26 – 27 Oct 2022. IEEE.

Sun, Q., Rizvi, G.M., Bellehumeur, C.T. and Gu, P., 2008. Effect of processing conditions on the bonding quality of FDM polymer filaments. *Rapid Prototyping Journal*.

Swirski, L. and Dodgson, N.A., 2013. A fully-automatic, temporal approach to single camera, glint-free 3D eye model fitting. *Proceedings of ECEM 2013*. https://www.researchgate.net/publication/264658852_A_fully-automatic_temporal_approach_to_single_camera_glint-free_3D_eye_model_fitting

The Ohio State University, 2020. *Warning Signs*. [online] Available at: <https://ehs.osu.edu/warning> [Accessed 16 September 2023].

Tobii Connect, 2022. *Tobii Pro Lab overview*. [online] Available at: https://connect.tobii.com/s/article/tobii-pro-lab-overview?language=en_US#:~:text=Tobii%20Pro%20Lab%20offers%20a,comparison%2C%20interpretation%2C%20and%20presentation [Accessed 20 February 2023].

Tobii, 2022. *Eye movement classification*, [online] Available at: https://connect.tobii.com/s/article/eye-movement-classification?language=en_US#:~:text=Tobii%20Pro%20Lab%20uses%20one,the%20same%20fixation%20or%20not [Accessed 2 March 2023].

Tobii, 2023. *Safety Guidelines*. [online] Available at: https://help.tobii.com/hc/en-us/articles/212372449-Safety-guidelines [Accessed 27 February 2023].

Tumer, E.H. and Erbil, H.Y., 2021. Extrusion-Based 3D Printing Applications of PLA Composites: A Review. *Coatings*, [e-journal] 11(4). https://doi.org/10.3390/coatings11040390

Vasavada, A.N., Danaraj, J. and Siegmund, G.P., 2008. Head and neck anthropometry, vertebral geometry and neck strength in height-matched men and women. *Journal of Biomechanics*, [e-journal] 41(1), pp. 114- 121. https://doi.org/10.1016/j.jbiomech.2007.07.007

Vishay, 2014. *High Power Infrared Emitting Diode, 940 nm, GaAlAs, MQW*. [online] 13 March. Available at: https://www.farnell.com/datasheets/2049675.pdf [Accessed 22 March 2023].

Wickramasinghe, S., Do, T. and Tran, P., 2020. FDM-Based 3D Printing of Polymer and Associated Composite: A Review on Mechanical Properties, Defects and Treatments. *Polymers*, [e-journal] 12(7). https://doi.org/10.3390/polym12071529

Zammarchi, G. and Conversano, C., 2021. Application of Eye Tracking Technology in Medicine: A Bibliometric Analysis. *Vision*, [e-journal] 5(4). https://doi.org/10.3390/vision5040056

Zhao, Z., Salesse, R.N., Marin, L., Gueugnon, M. and Bardy, B.G., 2017. Likability's Effect on Interpersonal Motor Coordination: Exploring Natural Gaze Direction. *Frontiers in Psychology*, [e-journal] 8. https://doi.org/10.3389/fpsyg.2017.01864

Zhu, Z. and Ji, Q., 2005. Robust real-time eye detection and tracking under variable lighting conditions and various face orientations. *Computer Vision and Image Understanding*, [e-journal] 98(1), pp.124 – 154. https://doi.org/10.1016/j.cviu.2004.07.012

APPENDICES

Appendix A: Figures

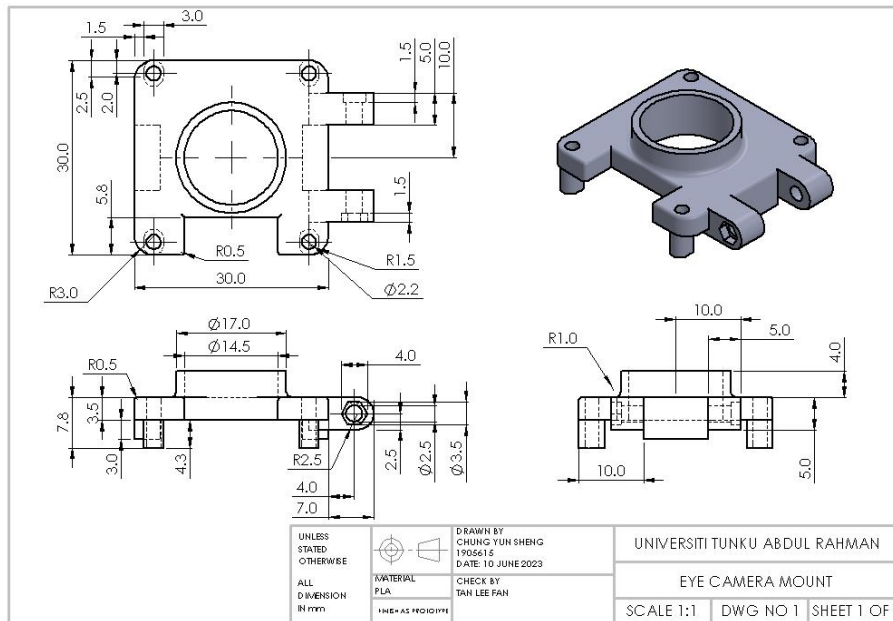

Figure A-1:Design Drawings for Eye Camera Mounting.
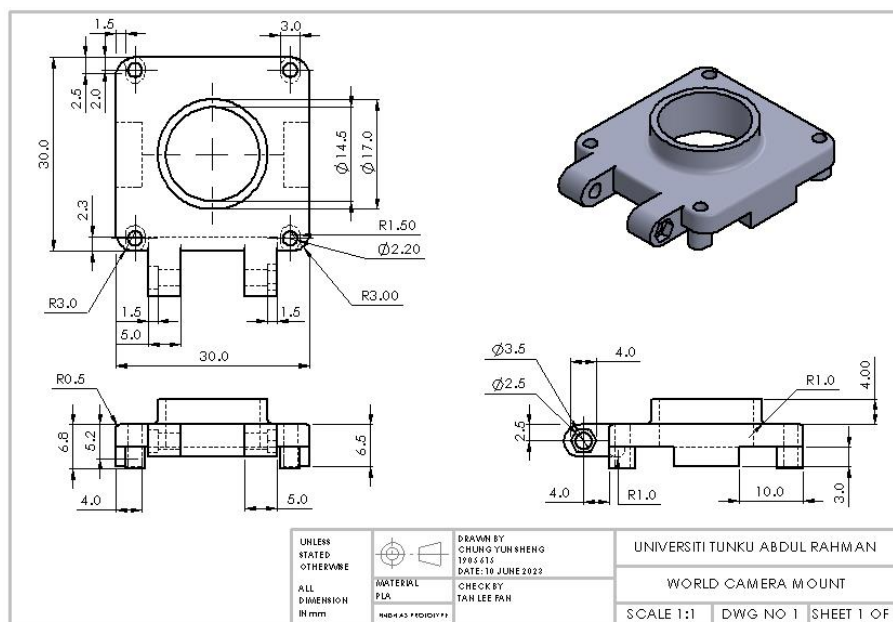

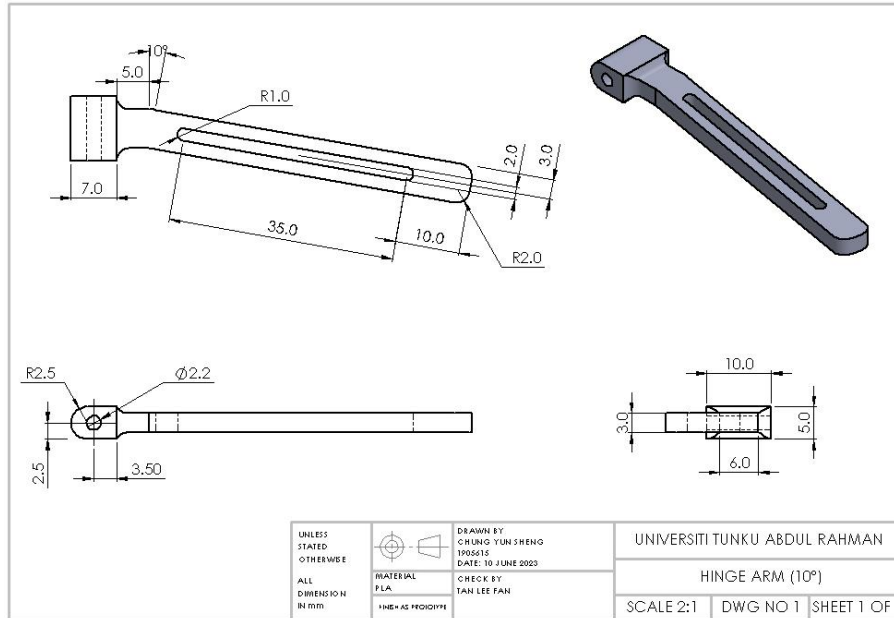Figure A-2: Design Drawings for World Camera Mounting

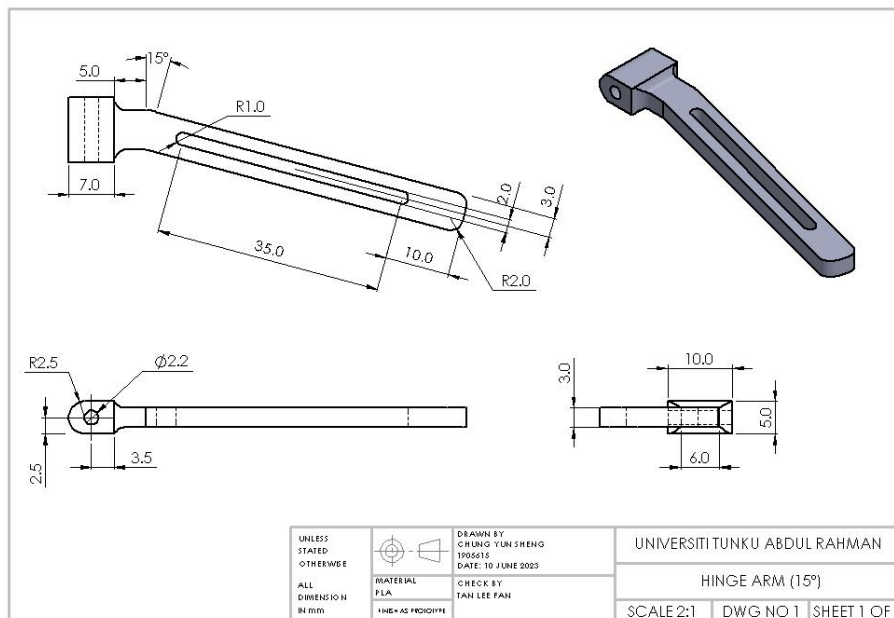Figure A-3: Design Drawings for Hinge Arm (10°).

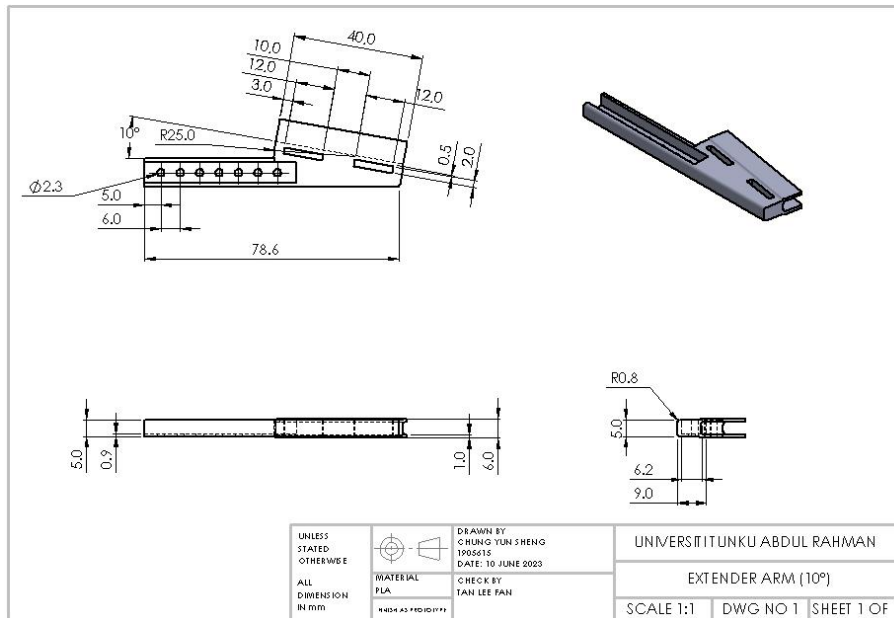Figure A-4: Design Drawings for Hinge Arm (15°).

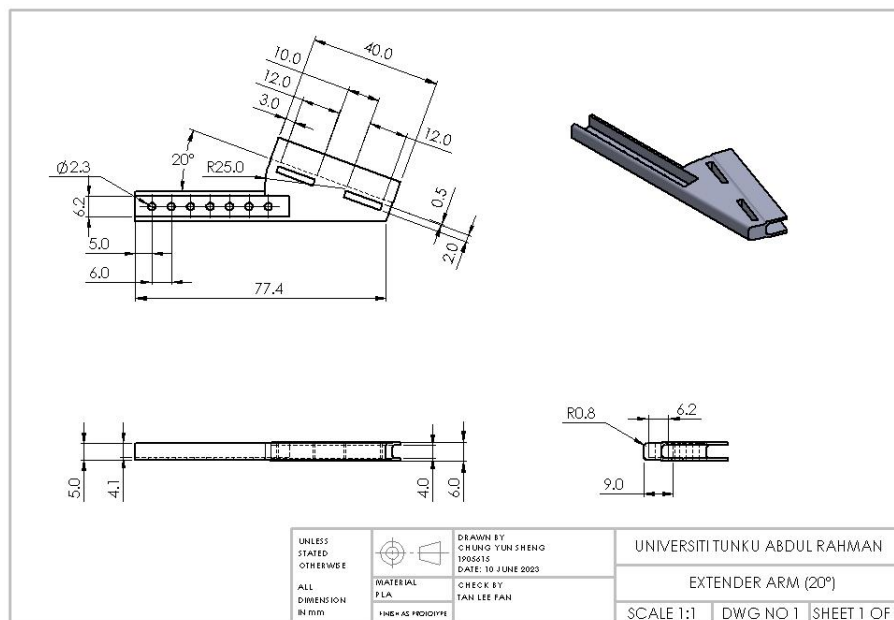Figure A-5: Design Drawings for Extender Arm (10°).

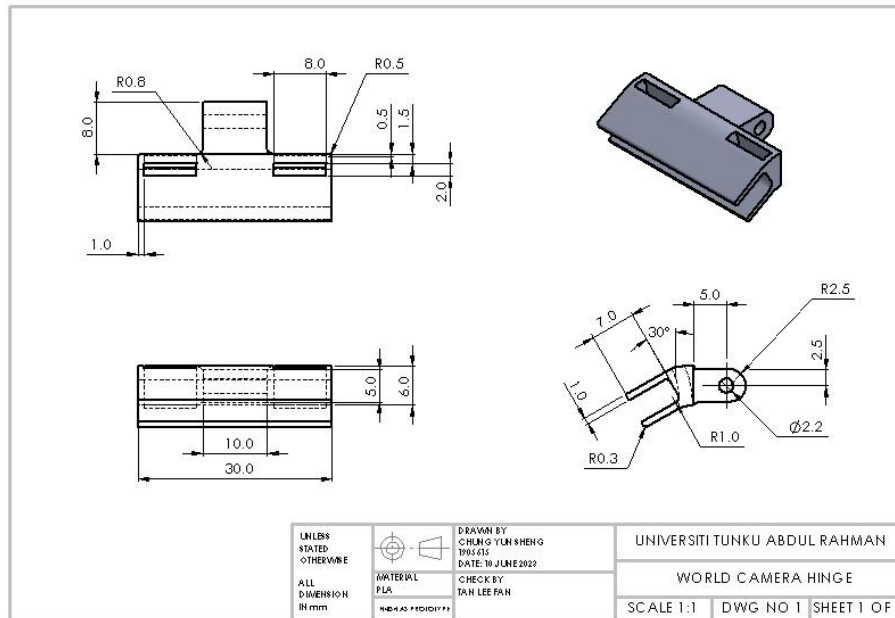Figure A-6: Design Drawings for Extender Arm (20°).
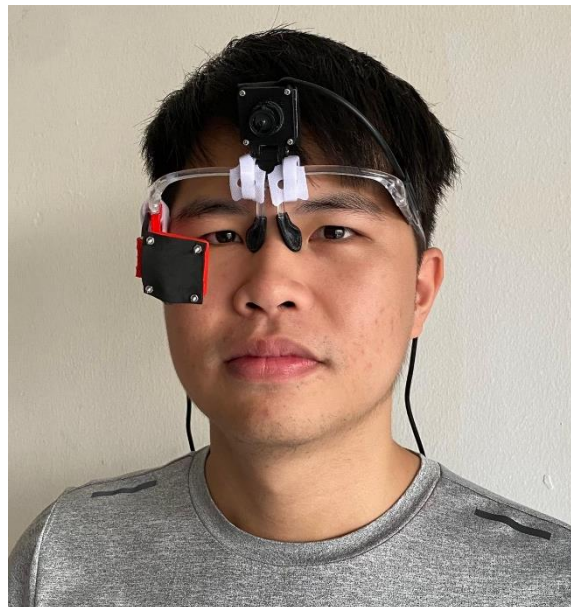
Figure A-7: Design Drawings for World Camera Hinge.

Figure A-8: Presentation of Developed Prototype on User.